

Arctic marine microbial ecology during the Svalbard Polar Night

—

Martí Amargant Arumí

BIO-3950 Master thesis in Biology - May 2018



Frontpage: R/V Helmer Hanssen in Ny-Ålesund, 9th of January 2017 at noon. Erin Kunisch

Acknowledgements

First and foremost, I want to thank my supervisor, Rolf Gradinger. Not only have you provided endless invaluable academic guidance, but you have given me the opportunity to take part in cruises that I could only have dreamed of, and the independence to face challenges head-on and come out a better scientist. Thank you for your patience with me, Rolf!

I would also like to thank my supervisor Aud Larsen for welcoming me to the Bergen microbiology group, letting me use their facilities and providing much welcome advice on flow cytometry and ecology. A big thank you to Lena Seuthe, who was an integral part in the design of this project in its early stages and gave invaluable help while packing for my first cruise.

Thanks also to the crew of R/V *Helmer Hanssen* for their work and assistance during the two cruises I took part in. To Hans-Matti Blencke who patiently taught me and let me use their flow cytometer, and this also extends to Ela in Bergen.

Thanks to all the SIZERs (Liza, Christine, Raph, Brandon, Ulrikke and Tobias) for all they have taught me either directly (life-saving R lessons! Great references!) or by being highly professional and fun to be around on a cruise and on dry land.

And thank you to all my office mates (Amalia, Néstor, Samuel, Domi, Asia, Emily-zoe and Adam) and UiT friends for all the wise advice, the laughs and the hearty meals (Erin!). To my parents, for their constant support to all my endeavors even though they keep me far away, and to Samuele.

Abstract

This study investigated the presence and activity of the components of the microbial food web (specifically viruses, heterotrophic bacteria and nanoflagellates, and autotrophic Cyanobacteria and pico-nanoflagellates) in the waters around the Svalbard archipelago (Norway) during the polar night period. The study focused on two major questions – are there differences in the community composition in different water masses? And, are there significant changes occurring during the polar night period? Two cruises in January and November 2017 with a total of 11 stations offered the opportunity to test these hypotheses. Flow cytometry was used to determine cell abundances in the uppermost 100m of the water column, and 8 serial dilution experiments were conducted to estimate their growth and grazing rates. All studied organism groups occurred in all samples in low abundances in both January and November. Comparison to the hydrographic regime revealed strong linkages between community structure and hydrography with higher abundances in Atlantic Water samples. Heterotrophic nanoflagellates and autotrophic pico-nanoplankton were markedly less present in January, whereas bacteria and viruses displayed steady concentrations in both months. This supported the hypothesis of succession in the microbial network throughout the polar night, and the possible role of mixotrophy and resting stages are discussed. No significant growth or grazing was detected in the experiments, which could be caused e.g. by low substrate availability and resting strategies. This study demonstrated that all members of the microbial food web organisms persists throughout the polar night in the major water masses around Svalbard. Future studies using alternative approaches are suggested to further study these processes during times of low activity.

Keywords: Svalbard, microbial loop, lower food web ecology, polar night, picoplankton, nanoplankton, viruses

Abbreviation list

ASW – Arctic Surface Water

AW – Atlantic Water

BSB – Barents Sea Branch

Chla – Chlorophyll *a*

CTD – Conductivity, Temperature, Depth sensor

DVM – Diel Vertical Migration

FSB – Fram Strait Branch

HNF – Heterotrophic Nanoflagellates

NAC – North Atlantic Current

NCC – Norwegian Coastal Current

PF – Polar Front

Pheo – Pheophytin

PNA – Pico- and Nanoautotrophs

Syn – *Synechococcus*

VBR – Virus to Bacteria Ratio

WSC – West Spitsbergen Current

Table of contents

Acknowledgements	3
Abstract	4
Abbreviation list	5
Table of contents	6
Introduction	7
Polar night	7
Planktonic groups of interest	9
Svalbard	10
Materials and methods	13
Sampling	13
Physical oceanography	14
Discrete chlorophyll (Chl) concentration sampling	15
Natural abundances of pico- and nanoplankton	16
Flow Cytometry	16
Statistical analysis	17
Serial dilution experiments	19
Protocol	19
Data analysis	19
Methodological considerations and disclaimer	20
Results	21
Physical oceanography	21
Photosynthetic pigments	22
Abundances of pico- and nanoplankton	25
Regional distribution	25
Depth distribution	28
Multivariate analysis.....	33
Serial dilution experiments	37
Discussion	39
Physical oceanography	39
Photosynthetic pigments	41
Abundances of pico- and nanoplankton	42
Multivariate community analysis	44
Serial dilution experiments	46
Methodological considerations	47
Conclusions and outlook	49
References	50

Introduction

Polar night

A polar night is a period of darkness that lasts for longer than 24 hours. This phenomenon takes place at latitudes polewards of the polar circles during the winter season both in the Arctic and in the Antarctic. The duration of this period increases with latitude, being maximum at the Poles, where there is only one sunset and sunrise every year. The irradiance during the polar night period is highly heterogeneous and can be classified into different categories. At latitudes between the Polar Circle ($66^{\circ} 33'$) and 72° the *civil twilight* prevails, with the sun staying less than 6° below the horizon. In these areas, darkness is still broken daily, even if the sun does not rise. Beyond $72^{\circ} 33'$ the *civil polar night* takes place, with no civil twilight daily as the sun stays between 6° and 12° below the horizon. At latitudes higher than $78^{\circ} 33'$, the *nautical polar night* prevails, with the sun more than 12° below the horizon. This is the northernmost light regime in which humans have placed settlements. At $84^{\circ} 33'$, the *astronomical polar night* sets in, during which there is no light detectable by human eye (Burn, 1996). The polar night spans a wide range of latitudes and is not a homogenous phenomenon in terms of duration and intensity throughout, which must be considered when studied as a physical factor for marine organisms (Berge et al. 2015).

Traditionally, the polar night has been thought to be completely devoid of light and biological activity. It is a long established fact that the photosynthetic reactions are strictly dependent on light intensity (Ryther, 1956). Under this premise, net photosynthetic growth during the polar night would become challenging if not impossible. The absence of primary production seemed to be concordant with diapause stages of several dominant Arctic marine copepod species (Kosobokova, 1999; Hirche, 1997), further preventing the transfer of energy to higher trophic levels and reinforcing the idea of a barren water column.

This paradigm has been challenged in recent years. As Berge et al. (2015) pointed out, “observations of the properties and processes occurring during the winter have been sparse and to a large degree opportunistic, [...] data have generally been restricted to fixed observatories, which lack important spatial resolution, or from freely drifting autonomous platforms, which compromises the repeatability necessary to quantify interannual variability”. These reports seem to indicate that the lack of observed biological activity during the Polar Night is more

related to the absence of consistent sampling efforts rather than to an actual resting period of all the ecosystem elements.

The polar night, even the nautical polar night, does not entail complete darkness for months. Still daily light cycles of biologically relevant ambient light exist with defined spectral composition, which certain groups of zooplankton might be able to detect down to 20-30m water depth (Cohen et al., 2015). Indeed, Berge et al. (2009) found evidence of Diel Vertical Migration (DVM) in both open and ice-covered waters, and Grenvald et al. (2016) detected migration patterns by zooplankton (presumably the euphausiid *Thysanoessa inermis*) in December-mid January. Aside from this ambient light which is present even in the darkest days of the year, several additional light sources have been proposed as drivers of the marine communities during this period. Last et al. (2016) proved that zooplankton change their vertical migration period to that of the lunar-day during winter, and that this pattern is modified both by the moon's phase and altitude above the horizon. Cronin et al (2016) reported that the depth at which the dim atmospheric light was substituted in intensity by bioluminescence coincided with a shift in the micro-mesoplankton community, hinting at an influence in the water column ecology during this period.

Overall, recent findings indicate that the polar night is not a uniformly dark period for the organisms living in the water column, and that key elements of these communities remain active, however with a main focus on larger zooplankton, while the microbial network largely remained unexplored in the winter season.

Planktonic groups of interest

Planktonic (from the Greek *πλαγκτός* (*planktos*), “drifter”) organisms are those that dwell in the water column and can not move against the water currents. They can be classified according to size (in logarithmic size classes) and trophic mode, according to whether they produce organic carbon from inorganic sources (Autotrophs) or they consume organic matter for energy production (Heterotrophs) (Figure 1). For the last few decades the focus has widened from the “classical” planktonic food chain, focused on the link between microphytoplankton, mesozooplankton and higher trophic levels to include what has been termed the “microbial loop” (Azam & Graf 1983). The contributing species in the microbial network come from a wide range of pro- and eukaryotic taxa. They are most abundant in terms of number and biomass in the world’s oceans and account for large fractions the oceanic production through their role as dissolved organic carbon and detritus recyclers (Børsheim 2017, Thingstad et al., 2008, Saint-Béat et al. 2018).

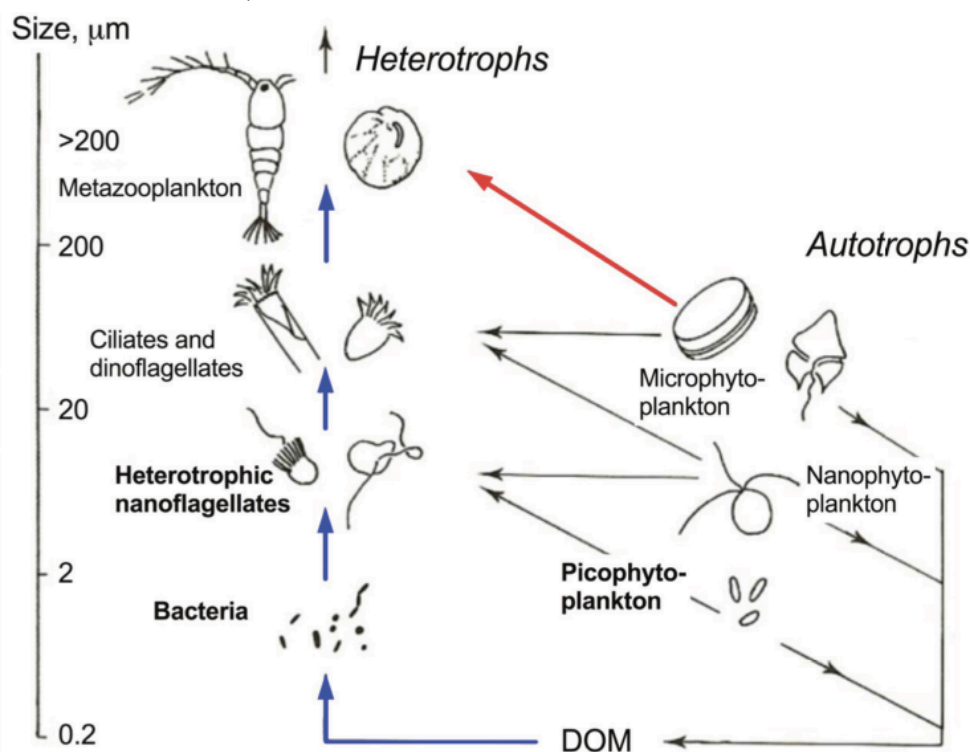


Figure 1: Simplified planktonic food web components (from Lund Paulsen et al. (2017), grouped by size class and trophic strategy. Arrows indicate trophic interactions. Dissolved Organic Matter (DOM) is a byproduct of the activity of all groups, and becomes the substrate for the bacteria that are at the base of the microbial loop (blue arrows). The “classical food chain” is represented by the red arrow. Note that some linkages like mixotrophy are represented in this schematic diagram.

The Pico- and Nanophotoautotrophs include eukaryotic pico- and nanophytoplankton, and Cyanobacteria. At high latitudes, these functional niches are mainly filled by often bloom

dominating diatoms plus the genera *Micromonas*, *Phaeocystis* and *Synechococcus*, which have also been found in Arctic waters during the polar night (Gradinger & Lenz, 1995; McKie-Krisberg and Sanders, 2014; Vader et al., 2015; Paulsen et al., 2016).

Heterotrophic pelagic bacteria are part of the picoplankton size fraction and consume dissolved organic carbon by osmotrophy. During the polar night, this carbon source is supposed to change from freshly and locally produced matter to preexistent or allochthonous sources, which are presumably more refractory and difficult to consume. Under such conditions, bacterial community composition might change and Archaea could become relatively more abundant due to their capacity to degrade more complex molecules as a source of carbon (Alonso-Sáez et al. 2008, 2012 and Wilson et al. 2016). The few published winter studies indicate low standing stocks of bacteria growing slowly during the winter period (Sherr & Sherr, 2003; Terrado et al., 2008, Rokkan Iversen & Seuthe, 2011).

The aforementioned groups are preyed upon by heterotrophic nanoflagellates (HNF, Christaki et al. 2001) through phagotrophy. This is a key step to make bacterial organic carbon accessible to higher trophic levels, as HNF can be consumed by ciliates, which again are of sufficient size to be food for copepods. This copepod-ciliate-flagellate trophic link has been found in many parts of the world's oceans (Calbet & Saiz, 2005), but few studies have addressed specifically the relationship between heterotrophic flagellates and picoplankton in the Arctic dark season (Vaqué et al., 2008).

Marine viruses, although not depicted in Figure 1, are important components of the microbial network. They are the most common biological in the seas, and occur in all aquatic environments, including polar seas (e.g. Fuhrmann 1999). Although understudied, they can cause mortality losses of picoplankton comparable to that of flagellate grazing (Suttle, 2007). Angly et al. (2006) observed that the Arctic virome contained a higher proportion of prophages (viruses that infect bacteria) than lower latitude seas, but viruses specialized in infecting cyanobacteria (cyanophages) were not strongly present, as neither were their hosts.

Svalbard

The North Atlantic Current transports warm and saline Atlantic Water northwards and splits into two branches when reaching the Barents Sea. The Fram Strait Branch (FSB) continues northwards towards the Svalbard archipelago, and it is named West Spitsbergen Current along the west coast of Spitsbergen. It interacts with waters on the shelf and in diverse fjords,

resulting in regionally differing physical conditions in each lower scale environment (Cokelet et al., 2008). Its influence reaches north of the Svalbard archipelago, where it starts sinking underneath the Arctic Surface Water (ASW), which is dominating the surface waters of the Central Arctic Ocean. Other processes at medium scales, such as eddies, also contribute to the dissipation of the Atlantic Water signature throughout the WSC (Crews et al., 2017).

The second branch of the NAC flows onto the shelf of the Barents Sea (Barents Sea Branch, BSB), progressively cooling until it meets the ASW at the Polar Front, where it submerges due to its higher density. As a consequence, the eastern coasts of the archipelago are influenced by much cooler, fresher water originating from the Arctic, while the west coast is dominated by warm Atlantic water (Bluhm et al., 2015).

This inflow of Atlantic Water is not constant throughout the year but subject to seasonal variability. Recent reports indicate that the inflow of warm and saline AW is greater during winter, and that it has been increasing in recent years (Grotefendt et al., 1998).

The extreme seasonality in air temperature, light regime and ice cover, coupled with the physical gradients generated by the interplay of water masses at regional and local scales, make the Svalbard archipelago an ideal area to study Arctic and North Atlantic pelagic communities and their resilience to the multiple stressors brought by global change. It is also the region where potentially northward expansion of more boreal species into the Arctic might occur, which has been observed for several key players of e.g. Barents Sea food webs (Frainer et al. 2017), but with a lack of focus on the interactions and relevance of the microbial network.

This thesis focused on the still largely unknown abundance and activity of mainly pico- and nanoplankton sized biota during the polar night, contrasting observational and experimental data gathered from different water masses with the following main research questions:

- How abundant are the components of the microbial food web in the waters around Svalbard during the Polar night period?
- How active are the aforementioned organisms? i. e. at what rate do small-sized planktonic organisms grow, and how intensely are they preyed upon?
- Are there significant differences between Atlantic and Arctic Water mass dominated areas?

And secondarily, elaborating upon the previous:

- What are the main drivers that shape this microbial community in the Polar Night? i. e. what determines the composition and dynamics of these communities?
- Can seasonal changes be detected within the dark winter period, comparing November with January data?

Materials and methods

Sampling

Sampling for this thesis was conducted during two research cruises onboard of RV *Helmer Hanssen*, in January and November 2017. The January expedition, labelled Polar Night Cruise 2017 (PNC17), was managed within the framework of the ArcticABC project (<http://www.mare-incognitum.no/index.php/arcticabc>) and included activities for several other projects. The November expedition (SIZE17) was organized by the UiT ArcticSIZE project (<http://site.uit.no/arcticsize/>).

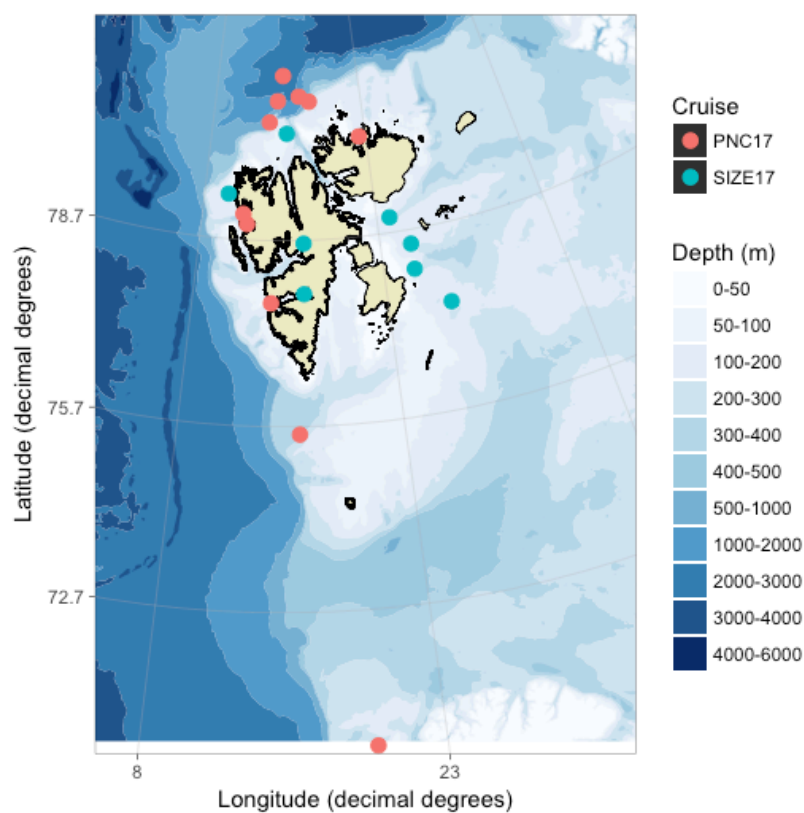


Figure 2: Map of the stations visited in both cruises.

CTD profiles and water samples were obtained in the Barents Sea, along the west coast of Spitsbergen (van Mijenfjorden, Isfjorden, Kongsfjorden and Krossfjorden), a transect along the shelf break north of Svalbard, Rijpfjorden and a transect on the shelf east of Spitsbergen (Figure 2, Table 1).

Table 1: Sampling stations overview with sampling depths for water samples

DATE	CRUISE	STATION NAME	LATITUDE	LONGITUDE	DEPTHS (M)	EXPERIMENT
4/1/17	PNC17	TB1	70.504N	19.609E	0, 5, 15, 50, 100	
6/1/17	PNC17	TB2	75.572N	16.082E	0, 5, 15, 50, 100	
7/1/17	PNC17	VMF9	77.690N	14.071E	5, 15, 50, 100	X
9/1/17	PNC17	KB3	78.953N	11.950E	5, 15, 50, 100	
10/1/17	PNC17	KF3	79.114N	11.597E	5, 15, 50, 100	X
11/1/17	PNC17	NS1	80.604N	13.664E	5, 15, 50, 100	
12/1/17	PNC17	NS5	80.947N	14.451E	5, 15, 50, 100	
12/1/17	PNC17	NS6	81.355N	14.986E	5, 15, 50, 100	X
13/1/17	PNC17	NS9	81.018N	16.596E	5, 15, 50, 100	
14/1/17	PNC17	NS10	80.931N	17.611E	5, 15, 50, 100	X
14/1/17	PNC17	R3	80.306N	22.256E	5, 15, 50, 100	
18/11/17	SIZE17	BF1	78.648N	16.664E	5, 15, 50, 100	X
18/11/17	SIZE17	W1	79.425N	10.206E	5, 15, 50, 100	
19/11/17	SIZE17	NS1_S	80.423N	15.342E	5, 15, 50, 100	X
19/11/17	SIZE17	B1	78.947N	23.972E	5, 15, 50, 100	
21/11/17	SIZE17	B2	78.471N	25.359E	5, 15, 50, 100	X
22/11/17	SIZE17	B3	78.062N	25.307E	5, 15, 50, 100	X
22/11/17	SIZE17	B4	77.434N	27.578E	5, 15, 50, 100	
24/11/17	SIZE17	VMF1	77.833N	16.601E	5, 15, 50, 100	

Physical oceanography

The CTD (Conductivity, Temperature, Depth probe) onboard of R/V *Helmer Hanssen* was a Seabird Electronics SBE 9, operated by the scientific crew on board (Hans Dybvik, UiT). The CTD provided water column profiles of conductivity, temperature and depth and in addition oxygen and chlorophyll fluorescence profiles at each station. The data were analyzed with the “oce” package (Dan Kelley, 2018) in the statistical computing software R. Temperature and salinity data were extracted and binned (averaged) for every meter of the water column. The resulting dataset was used to construct vertical profiles of temperature, salinity and biological data and formed the basis for multivariate statistics (see below).

Discrete chlorophyll (Chl) concentration sampling

Analyzing the quantity and quality of the photosynthetic pigments present in the water column during the Svalbard polar night was not the main objective of this thesis. Therefore, sample collection during both cruises was done by Coralie Barth-Jensen and Peter Glad (AMB-UiT) for PNC17, and by Christine Dybwad (AMB-UiT) and Hanna Böpple (UiB) during SIZE17. Samples were jointly analyzed with the above mentioned colleagues in the laboratory analysis.

On both cruises, water was subsampled from 5 Liter Niskin bottles into plastic containers. A known volume (1L on SIZE17 and around 0.6L on PNC17) was filtered onto GF/F filters (0.7 µm pore size), which were stored in the dark at -20°C until analysis.

Pigment analysis was carried out according to Holm-Hansen & Riemann (1978). The filters were thawed and placed on a test tube. Five mL of pure methanol were added to the filter and left to incubate overnight (12-16 hours) at 4 °C. The methanol acts as an organic solvent and extracts the chlorophyll from the cells and other structures that have been retained on the filter. The time needed to extract practically all the chlorophyll from the sample has been subject of discussion in past years, and recent findings suggest that the extraction time had no significant influence within a range of 3 to 24 hours, but that might be dependent on the solvent used (Wasmund et al. 2006).

After extraction, the pigment fluorescence of the methanol solution was measured using a Turner 10-AU-000, last calibrated in August 2017. The methanol solution contains both active chlorophyll and its analogue pheophytin, which lacks a Magnesium ion at the center of its hemo group. After the first fluorescence reading, two drops of 10% HCl were added to the tube, which transforms the chlorophyll molecules into pheophytin. The difference between the two readings before (R_b) and after (R_a) acidification was used to calculate the amount of chlorophyll a (Chl a) and pheophytin (Pheo) present in the sample.

$$Chl_a \left[\frac{mg}{m^3} \right] = Tau \times F_d \times (R_b - R_a) \times \frac{V_m}{V_f};$$

$$Pheo [mg/m^3] = Tau \times F_d \times (2.839 \times R_b - R_a) \times \frac{V_m}{V_f}$$

where F_d and Tau are factors estimated during the calibration of the fluorometer, V_m is the volume of methanol added to the sample and V_f is the volume of filtered sample.

Natural abundances of pico- and nanoplankton

Flow Cytometry

Water was sampled from 5 L Niskin bottles mounted on the same chassis as the CTD. As a general rule, water was sampled from 5, 15, 50 and 100m depth (Table 1). The water was poured into 60mL dark glass bottles through a silicone tube wrapped in tape to prevent light exposure. The bottles were rinsed three times with sample water by inversion before the final filling. Immediately after handling, the bottles were transported inside a cooler to a dark laboratory. The remaining procedures were carried out in darkness with the help of a headlamp with green or red light.

Under the fume hood, three 2mL cryovials and two 5mL cryovials were filled with 1.9mL and 4.9mL of sample (respectively). 25% filtered glutaraldehyde solution was added to the vials: 38 μ L in the 2mL vials and 98 μ L in the 5mL samples. The samples were then wrapped in aluminum foil and kept in the dark and cold (in a fridge, around 4°C) for no less than 2 hours. On PNC17, the vials were placed in nylon bundles and frozen by placing inside a dry shipper for 1 minute. The bundles were then placed in the on-board -80°C freezer. On SIZE17, the samples were frozen by immersion in liquid nitrogen and stored in the -80°C freezer. This procedure was repeated without variation for all the flow cytometry samples.

The January samples were frozen in the dry shipper because the access to the liquid nitrogen tanks on board proved difficult due to remarkably bad weather. This caused complications for the transportation of the samples, as the dry shipper was not cold enough due to being used so often. Some of the samples thawed on the way back to UiT, but in all cases there existed backup samples (the main bulk remaining in the -80°C freezer on the vessel) and thus no information was lost.

Cytometric analysis of the PNC17 samples was conducted at the University of Bergen (UiB), in the Marine Microbiology research group facilities. Abundances were determined on an Attune Acoustic Focusing Flow Cytometer (Applied Biosystems by Life technologies) with a syringe-based fluidic system and a 20mW 488nm (blue) laser, equipped with detectors for forward and side scatter as well as green, orange and red fluorescence. This allowed to determine not only the amount of cells present in the sample but also their relative size and contents of chlorophyll *a*, phycoerythrin and/or the quantity of DNA (through staining with SYBR Green-1). The SIZE17 samples were analyzed at UiT (NFH), with a Cyflow Cube 8 (Partec) cytometer using the same approach.

Typical scatter plots of the sample run are shown in Figure 3. Depending on the groups of interest for the research, different variables can be selected for the plots: side and back scatter are a proxy of cell size¹, and the different wavelengths of fluorescence report the presence of various pigments. When analyzing these plots, certain ranges or “gates” are used as the signal for a particular group (i.e. bacteria) and used to create an output file with the abundance of cells present in each gate.

The biological data collected were grouped in the following main compartments: Heterotrophic nanoflagellates, autotrophic pico- and nanophytoplankton, heterotrophic bacteria, cyanobacteria and viruses.

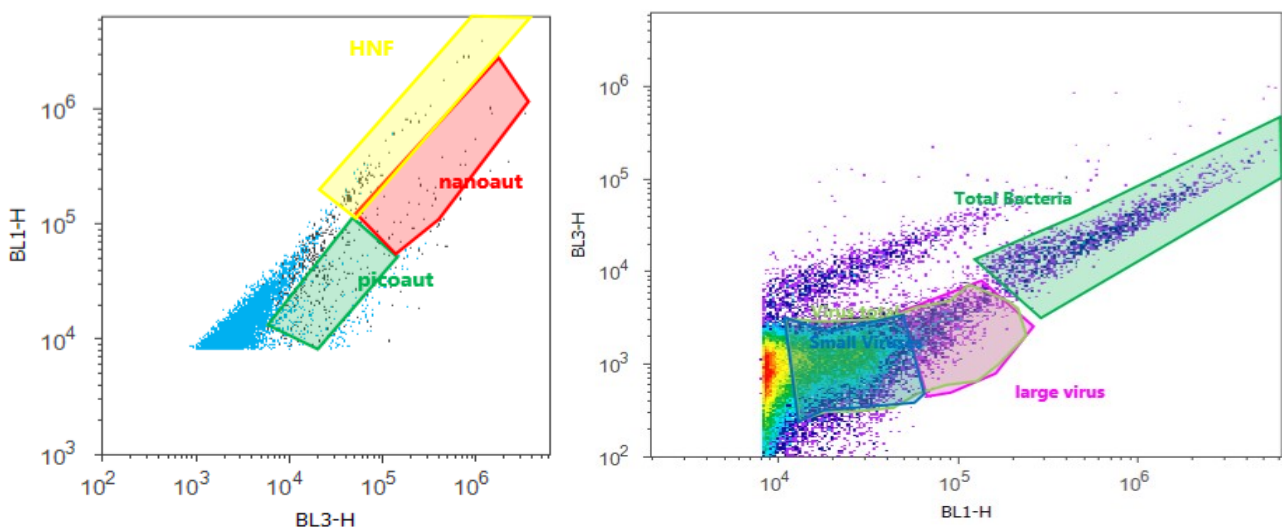


Figure 3: Scatterplots of the cytometric analysis of a sample. BL1-H represents green fluorescence (DNA stained with SYBR Green-1) and BL3-H is proportional to red fluorescence (chlorophyll presence). The overlying polygons are the “gates”, the groups of readings considered to represent a consistent unit of study

Statistical analysis

Tests. One-way ANOVA tests ($\alpha=0.05$) were performed to compare a single variable among discrete levels, specifically chlorophyll *a* concentration or concentration of the aforementioned biological groups between stations.

For the overall community analysis, several tools from multivariate statistics were required.

PCA. Principal component analysis was performed on the biological data (abundances of each group in each sample). It is a useful tool to reduce the dimension in a multivariate dataset, as it finds linear combinations of the different variables that explain the maximum amount of

¹ There have been reports of some groups of microalgae that might increase their side or backscatter for reasons other than their size, such as the calcium carbonate scales of Prasinophytes (Aud Larsen pers. comm.).

variance. It is not a hypothesis-test based method, but a useful tool in visualizing microbial community structure. Once the samples were allocated in the PCA biplot, they were grouped according to the water mass they belonged to. The water masses were defined as Atlantic Water (1-4°C, 34-35psu), Arctic Surface Water (below 0°C and 28-33psu), and mixed water in fjords influenced by processes such as sea ice melting/formation or terrestrial runoff (Coachman and Barnes 1962).

Non-metric Multidimensional scaling. Non-metric multidimensional scaling (NMDS) is a tool for visualizing how samples group together in a multidimensional space., based on a distance matrix. The distance between all samples is calculated using the index that better suits the dataset's characteristics, and a matrix of these distances is built. From there, the samples are placed in a low-dimension space that best maintains these distances. When the distance or dissimilarity index chosen by the researcher is non-Euclidean, such as the Bray-Curtis dissimilarity, the technique aims to represent the *ordering* (how similar two samples are in contrast to how similar they are to others) rather than the distance between samples.

$$b_{ii'} = \frac{\sum_{j=1}^J n_{ij} - n_{i'j}}{n_{i+} + n_{i'+}}$$

The Bray-Curtis measure used in this study is a good fit for analysis of absolute counts in samples of the same volume or size, which is the case of this project's dataset (Greenacre & Primicerio, 2013). Bray-Curtis is also considered easy to interpret in community analysis because it ranges from 0 (identical samples) to 100 (completely different). *A posteriori*, the temperature and salinity of each sample were fitted to the biplot to see the effect of these physical variables on the ordination of the communities, and the samples were grouped according to water mass as it was done with the PCA biplot (see Results).

Cluster analysis. Clustering the samples is an alternative way to visualize the data upon which an NMDS is based. Instead of distributing them in a two-dimensional space, a hierarchical clustering aims to produce a dendrogram where the distances between samples are clearly displayed. The starting point is once again the Bray-Curtis dissimilarity matrix. To build the tree, the two closest samples are linked through a node in the tree, and subsequently the most similar sample to each new cluster is added. It is not uncommon to display this technique together with a NMDS of the same data, as their joint interpretation may aid in the definition of groups and patterns (Vihtakari et al. 2018).

All three multivariate methods were implemented using the “vegan” package (Oksanen et al 2009) in the statistical analysis software R.

Serial dilution experiments

Protocol

Serial dilution experiments were conducted according to the original procedure described by Landry and Hassett (1982). Water samples from 15m water depth were taken by CTD-mounted Niskin bottles and transported in a container covered by a double layer of black plastic to avoid any light incidence.

The water was diluted (1.0, 0.75, 0.5, 0.1, 0 fractions) with sample water previously filtered through 0.2µm polycarbonate filters and distributed into 250mL cell culture bottles. Each dilution incubation was done in triplicated, and all the bottles were kept inside black boxes in a dark cold room on board of RV *Helmer Hanssen* at 0-2°C. The temperature inside of the boxes was monitored using HOBO Pendant[®] Temperature/Light data loggers during PNC17, and by routinely checking the cold room thermometer in SIZE17.

A total of eight experiments were done, the incubations running no shorter than 96 hours as suggested by Pree et al. (2016). The bottles were inverted manually twice a day during incubations to evenly redistribute particles. Time-0 samples were taken at the start of the experiment for the 100% and % SW dilution steps (only during SIZE17, see *Disclaimer*), and for all the steps at the end of the experiment. These samples were quantified following the protocols described above for flow cytometry.

Data analysis

Landry and Hassett first described that this experimental setup allows to simultaneously estimate two rates in planktonic trophic relationships if three major assumptions were met:

- The growth of individual prey cells (phytoplankton or bacteria) was not modified by the presence of others, e.g., nutrients are not limiting.
- The probability of being predated on is a function of the encounter rate between predator and prey cells.
- The prey cells are growing exponentially and thus the stock can be described by the following equation:

$$N_t = N_0 \times e^{(k-g)t}$$

in which N_t is the stock of cells at a given time t , N_0 is the initial stock, k is an instantaneous coefficient of population growth and g is an instantaneous coefficient of grazing. In the experiments, it is possible to measure all the variables of the equation to calculate the term $(k - g)$:

$$(k - g) = [\ln \left(\frac{N_t}{N_0} \right)] / t$$

which is then plotted against the dilution factor in a linear regression. Because k is independent of the dilution and g is directly modified by it, the slope of the resulting regression line is an estimate of g and the intercept in the y-axis can be used to approximate k .

The applicability of this method and the validity of the assumptions in the light of this thesis' results is argued in the *Discussion* section.

Methodological considerations and disclaimer

During the Polar Night Cruise in January 2017, a methodological oversight led to the absence of time-0 samples at the 0% seawater dilution level. Effectively, this means that 4 out of the 8 experiments lack blank t-0 controls.

Assuming a very conservative generation time of 10 days for bacteria (Sherr & Sherr 2003, Rolf Gradinger *pers. Comm.*), the initial stock in the different bottles was estimated using the equation displayed above, and the remaining parameters calculated accordingly. The results did not seem to vary greatly from those obtained when assuming a generation time of 7 or 20 days, which led to the conclusion that this oversight is not greatly affecting the totality of the experimental effort.

At the same time, because the protocol for the 4 experiments during SIZE17 was identical and in this occasion blanks were taken properly, the time-0 concentrations for the second set of experiments were compared with the first ones and were found to be in the same range, validating our assumptions.

Results

Physical oceanography

Temperature and salinity showed wide variations during the November and January expeditions (Figure 4) covering similar temperature ranges with values between below -1°C to over 4°C . Salinities were highest at the warmest stations with values close to (January) or exceeding 35.

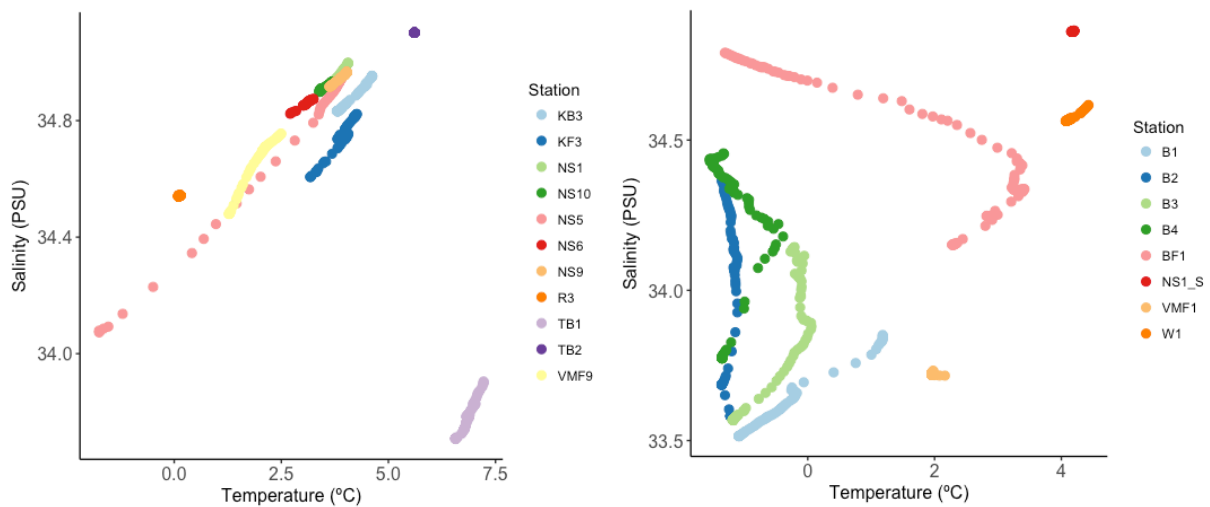


Figure 4: Temperature – Salinity diagrams for the uppermost 100m of the sampling stations.

The temperature and salinity variation was typical for the various water masses occurring in the study area. Strong influence of Atlantic Water (AW) inflow was found at the Barents Sea stations TB1 and TB2, with water temperatures between 5°C and 7°C . The lower salinity at TB1 is indicative of the influence of the fresher Norwegian coastal current, while TB2 had typical AW salinities (35.1).

Along the western and northern side of Svalbard, the Atlantic influence noticeably diminished. The stations on the shelf west of Svalbard and in fjords were colder (0 to 5°C) and generally fresher (<35) than AW with high variability. North of Svalbard at the “NS#” stations transect this cooling trend continued. Rijpfjorden was significantly colder (0.1°C) but not fresher (34.5) than the aforementioned stations.

The “B#” stations were located east of the Svalbard archipelago and north of the Polar front and were sampled in November. Average temperatures for these stations were below 0°C and salinity was low with values between 33.6 and 34.1.

Based on the temperature and salinity characteristics (Figure 4) and the known water mass distribution in the area (see introduction), I classified each station into one of the following categories using both location and T/S data²:

- Norwegian Coastal Current: Station TB1.
- Atlantic Water: Station TB2.
- West Spitsbergen Current: Stations VMF1, VMF9, BF1 (surface water), KB3, KF3, W1, NS1, NS5 (bottom water), NS6, NS9, NS10.
- Arctic Surface Water: Stations BF1 (bottom water), NS5 (surface water), R3, B1, B2, B3, B4.

Based on standard definitions of Arctic water only the B# transect stations and the surface (first 15m) of NS5 represent true Arctic Water (temperature below 0 and salinity between 28-34). The higher salinity present in the surface water of BF1 and the water column at R3 indicates that they are actually cooled Atlantic Water masses. However, given the significance of temperature for the development and composition of communities around Svalbard, they have been assigned to the Arctic Water category.

At most stations the water columns were vertically not stratified in the uppermost 100m of the water column and only stations BF1 and NS5 were stratified with a layer of colder and fresher water over warmer and saltier water Atlantic Water.

Photosynthetic pigments

Photosynthetic pigments concentrations (Figure 5) were overall very low, but nonetheless detectable all around the Svalbard archipelago both in November and in January. At all stations and depths, chlorophyll *a* (Chl*a*) and pheophytin (Pheo) concentrations were below 0.1mg/m³, with most data between 0.01 and 0.05mg/m³.

² “Norwegian Coastal Current” and “West Spitsbergen “Current” are not water masses *per se*, as essentially they contain Atlantic Water that flows along the coasts of Norway and Spitsbergen respectively. However, because throughout this movement this water undergoes changes that are relevant for the microbial communities they contain, the current names have been used as a placeholder for water masses.

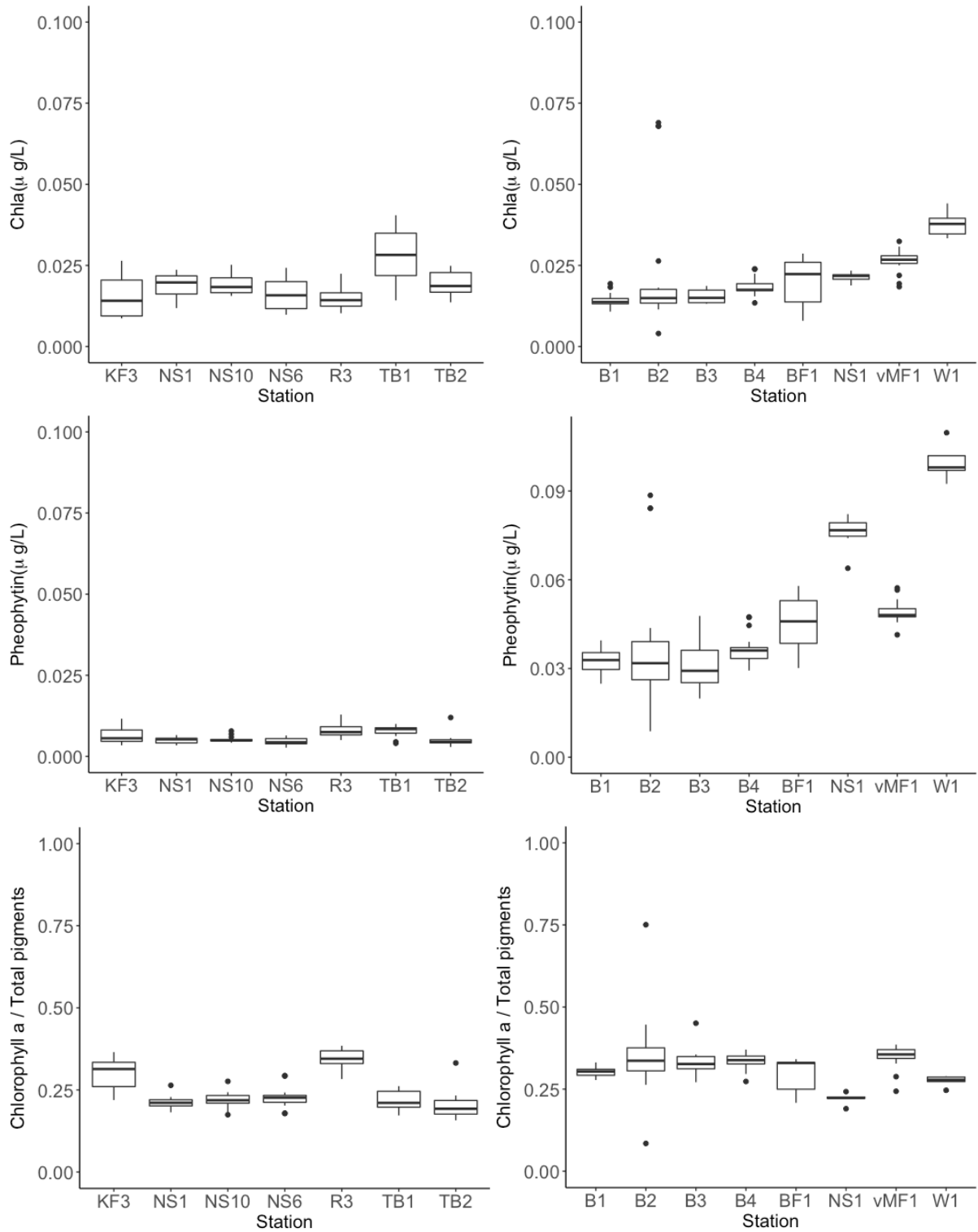


Figure 5: Photosynthetic pigment concentrations. The boxes depict all the data points contained within the first and third quartile, and the whiskers extend to 1.5 times the variance contained in the box. Data outside of this range is plotted as an outlier, and this applies to all boxplots in this thesis. Top: Chla concentration ($\mu\text{g/L}$) in January (left) and November (right). Middle: Pheo concentration ($\mu\text{g/L}$) in January and November. Bottom: Chla to total pigments ratio in January and November.

Although overall low, November concentrations of Pheophytin (Pheo) significantly exceeded the January concentrations ($p < 0.05$). No significant difference was found for Chl a ($p > 0.05$).

Regionally, Chl a concentrations were highest at stations influenced by Atlantic water. In January, station TB1 presented significantly higher values ($p < 0.05$) as did stations W1 and VMF1 in November. The exceptionally high Chl a and Pheo concentrations at station B2 at 50m depth (Figure 5) were consistent between sample replicates and also supported by high vertical flux rate at this depth (Christine Dybwad *pers. Comm.*). Similar regional differences were found for Pheo concentrations (Figure 5), which were significantly higher at the western and/or Atlantic Water influenced stations in November (W1, VMF1 and NS1, $p < 0.05$). No such difference was detectable in January ($p > 0.05$).

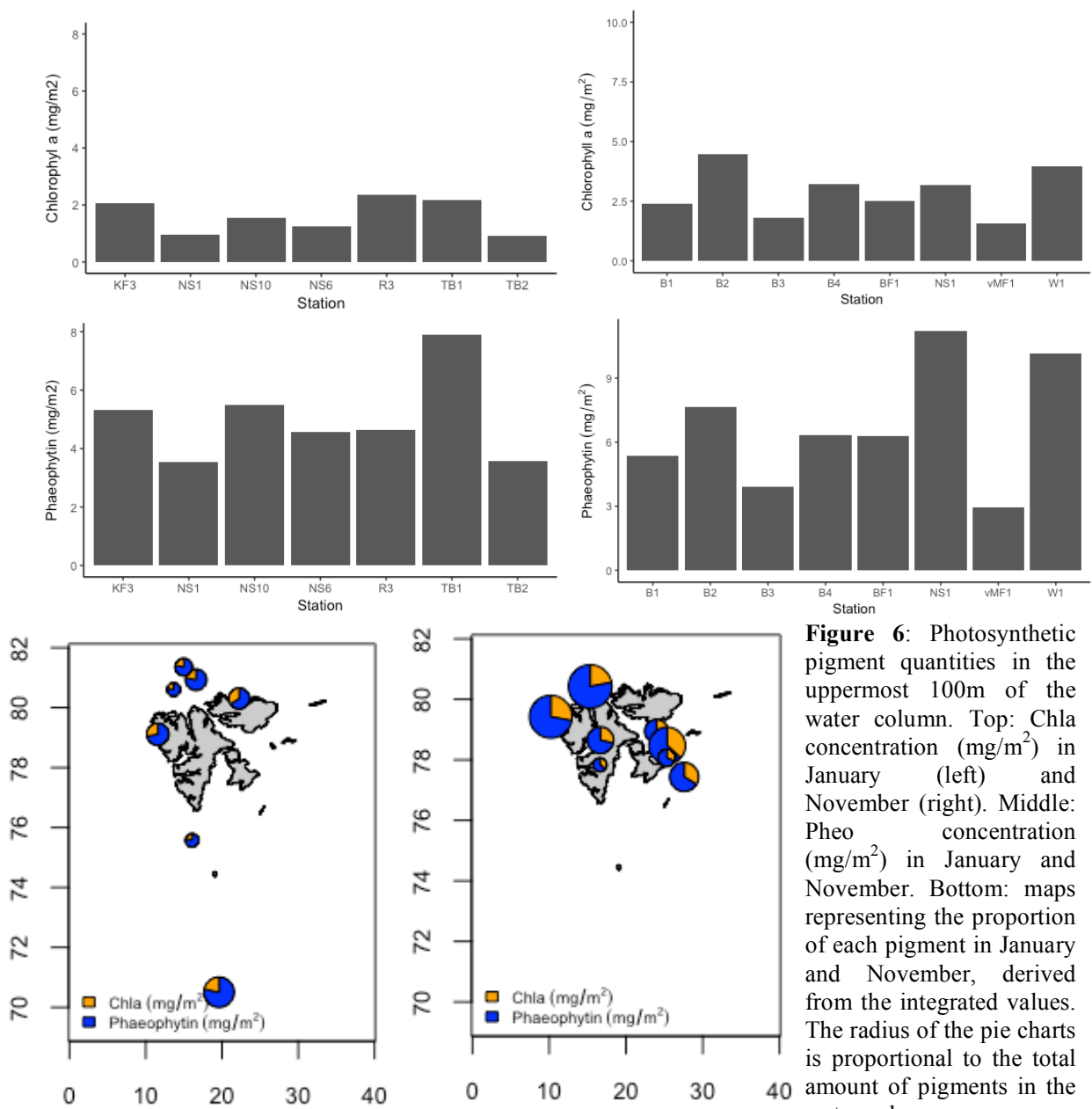


Figure 6: Photosynthetic pigment quantities in the uppermost 100m of the water column. Top: Chl a concentration (mg/m 2) in January (left) and November (right). Middle: Pheo concentration (mg/m 2) in January and November. Bottom: maps representing the proportion of each pigment in January and November, derived from the integrated values. The radius of the pie charts is proportional to the total amount of pigments in the water column.

The ratio of Chl*a* to the total amount of pigments (Chl*a* plus Pheo, Figure 5) was low at all stations in November and in January and did not exceed 0.5, with the exception of the 50m sample at station B2 with a ratio of 0.75. Although overall low, Chl*a* contributed significantly more to total pigment concentration in November (mean ratio: 0.32) compared to January (mean ratio: 0.24, $p < 0.05$). In January, two stations (KF3 and R3) showed significantly higher ratios than the rest of stations ($p < 0.05$). In November, the ratio in station NS1 was significantly lower than the rest ($p < 0.05$).

Integrated Chl*a* and Pheo concentrations for the uppermost 100 m of the water column were below 12 mg/m^2 at all stations (Figure 6). November values for both Chl*a* and Pheo (mean 2.88 mg/m^2 , 6.73 mg/m^2) were greater than the those in January (1.73 mg/m^2 , 5.24 mg/m^2) ($p < 0.05$), nonetheless with increased variability between stations. TB1 Pheo values (7.9 mg/m^2) exceeded those of the rest of stations in January, and the same can be said for NS1 (11.20 mg/m^2) and W1 (10.16 mg/m^2) in November. Overall, Pheo concentrations were about 2-3 times larger than for Chl*a* (Figure 6 bottom).

Abundances of pico- and nanoplankton

Regional distribution

Pico- and Nanophytoplankton (PNA).

Phototrophic pico- (size range 0.2 to $2 \mu\text{m}$) and nanoplankton (size range 2 to $20 \mu\text{m}$) was observed during both expeditions with distinct differences related to region/water masses and to season.

In January, small autotrophic organisms were present in a concentration ranging between 10 and 50 cells/mL with a mean value of 22.1 ± 12.4 cells/mL (Figure 7). Highest concentrations occurred at the stations TB1, VMF9 and the surface waters of station NS5 with values approaching 50 cells/mL.

The November concentrations of PNA were significantly above the January data ($p < 0.05$) with an average of 1385.1 ± 2055.8 cells/mL. Highest concentrations were found in the western fjords, specifically the innermost part of Van Mijenfjorden (VMF1) with concentrations exceeding 6000 cells/mL, causing the high standard deviation stated above. The stations located in the WSC category showed similar abundances to those found in Arctic waters.

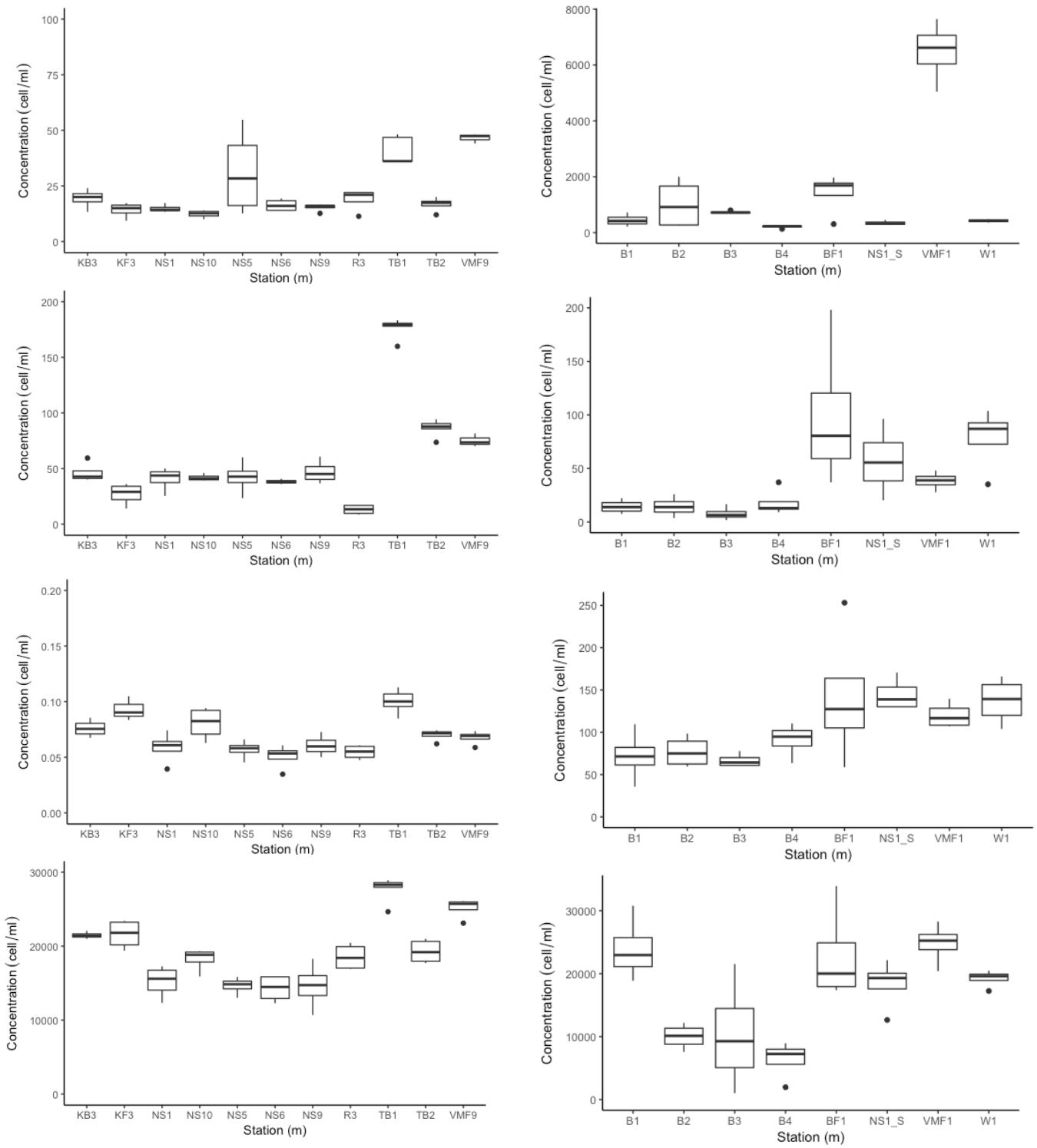
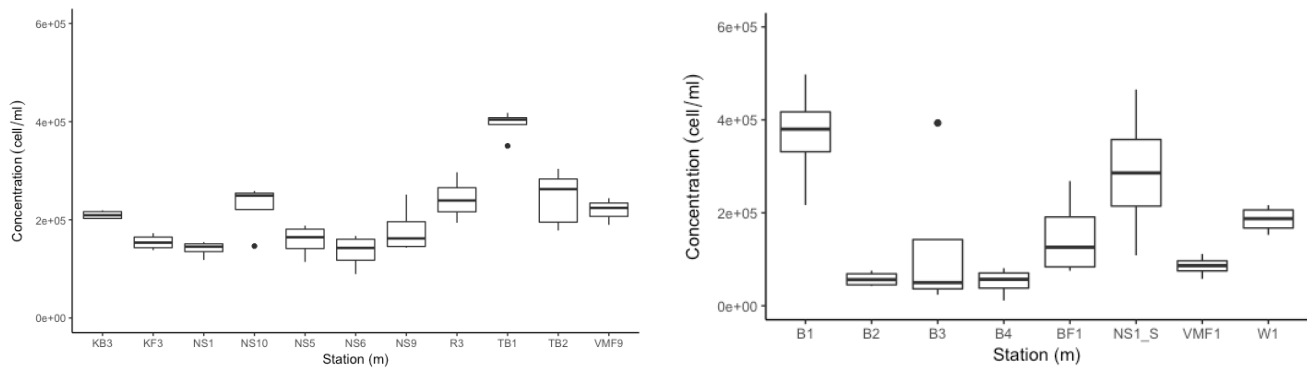


Figure 7 (continues on next page): Microbial organisms abundances per unit of volume in the sampled stations, in January (left) and November (right). From top to bottom: PNA, *Synechococcus*, HNF, Bacteria, Viruses (next page)



Cyanobacteria. In January, photoautotrophic prokaryotic organisms in the picoplankton size range, presumably belonging to the genus *Synechococcus*, were detected along the west and north coast of Svalbard at concentrations of 60.5 ± 46.4 cells/mL (Figure 7). Highest abundances occurred in the Barents Sea (TB1, 2) and the southernmost fjord (Van Mijenfjorden, VMF9) while Rijpfjorden R3 had the lowest abundance below 30 cells/mL.

In November, a similar range of concentrations was observed with overall 20 to 200 cells/mL, averaging 40.9 ± 41.7 cells/mL. The four stations in the Barents Sea B1-4 dominated by ASW had significantly lower abundances of cyanobacteria ($p < 0.05$) compared to the stations affected by Atlantic Water inflow (BF1, W1, NS1_S and VMF1).

Heterotrophic nanoflagellates (HNF). In January, concentrations of this functional group ranged between 0.05 and 0.15 cells/mL, average 0.07 ± 0.02 cells/mL (Figure 7). The northernmost stations on the shelf and in Rijpfjorden had lower concentrations compared to the Barents Sea and the western fjords stations. Highest January abundances of HNF occurred at the southern and Atlantic Water/Norwegian Coastal Current influenced station TB1.

The concentrations of HNF in November were significantly higher than in January ($p < 0.05$) with abundances ranging between 50 and 200 cells/mL (average 106.3 ± 44.0 cells/mL). A similar regional and water mass related distribution was observed for HNF as seen for cyanobacteria with lowest abundances at the Barents Sea stations B1-4.

Bacteria. In January, heterotrophic bacterial abundances ranged between 1 to $3 \cdot 10^4$ cells/mL (average $19.3 \pm 4.7 \cdot 10^3$ cells/mL). Similar to HNF, lowest abundances occurred along the northern transect, specifically at stations NS5-9 while highest abundances occurred at TB1.

In contrast to HNF, bacterial abundances in November were not significantly different to the January data ($p > 0.05$) with abundances ranging from $1.0 \cdot 10^3$ to $3.4 \cdot 10^4$ cells/mL (average $1.7 \cdot 10^4 \pm 8.1 \cdot 10^3$ cells/mL). Abundances on the western Atlantic water influenced stations

were consistently high. In the Barents Sea, a strong decline was detectable from high values at B1 south of Hinlopen Strait towards the south (B2 -4).

Viruses. Abundances of viruses ranged in January between 8.9×10^4 to 4.2×10^5 viruses/mL (average $2.1 \times 10^5 \pm 8.2 \times 10^4$ viruses/mL). While no clear relationship between their abundances to water masses or region could be detected, station TB1 had the highest concentrations with a mean of $3.9 \times 10^5 \pm 2.6 \times 10^4$ viruses/mL.

Similar to heterotrophic bacteria, cyanobacteria and HNF, viruses were more abundant in the Atlantic Water stations ($1-3 \times 10^5$ viruses/mL) compared to the Barents Sea (B2-4). Station B1 not only exceeded the more southerly stations but had the highest virus concentrations encountered at all stations ($3.7 \times 10^5 \pm 1.2 \times 10^5$ viruses/mL).

Depth distribution

The vertical distribution of all functional groups as well as the vertical gradients in temperature and salinity throughout the uppermost 100 m of the water column in January 2017 are shown in Figure 8a-k. As already stated above, most stations were not stratified at the time of sampling indicating a strong mixing regime extending down to at least 100m. Therefore, the large differences in temperature and salinity seen during the expedition (Figure 3) were driven by regional water mass characteristics and not local stratification. The vertical distribution of biota (Figure 8) followed the distribution of temperature and salinity with very limited vertical differences. At the few stations with weak vertical gradients in physical variables (TB1, VMF9, KF3), highest concentrations of cells from all functional groups were found within the uppermost 15m of the water column. Only NS5 showed a very distinct vertical stratification with low salinity Arctic water in the upper most 20m separated by a strong pycnocline from warm Atlantic water. At this station, abundances of nanophytoplankton (from 30 to 10 cells/mL) decreased sharply from the surface layer to the waters below the pycnocline. Other taxa did not follow the same trend.

Stations sampled in November (Figures 8l-s) also showed a well mixed and poorly stratified water column structure, specifically at the stations within the WSC. The vertical structure in Billefjorden (BF1) showed vertical gradients for both temperature and salinity, with water getting colder and more saline below 40 to 60m water depth. Contrastingly, the Barents Sea stations B1-4 displayed sharp gradients of temperature and salinity below a surface mixed layer. Strongest gradients were visible at B2-4, suggesting the presence of a pycnocline. These gradients were of varying slopes with B1 being the least stratified. Most biota was evenly

distributed within the water columns at the November stations. However phototrophic pico- and nanoalgae showed a strong decrease from the colder and less saline surface waters into the warmer water below 40m water depth.

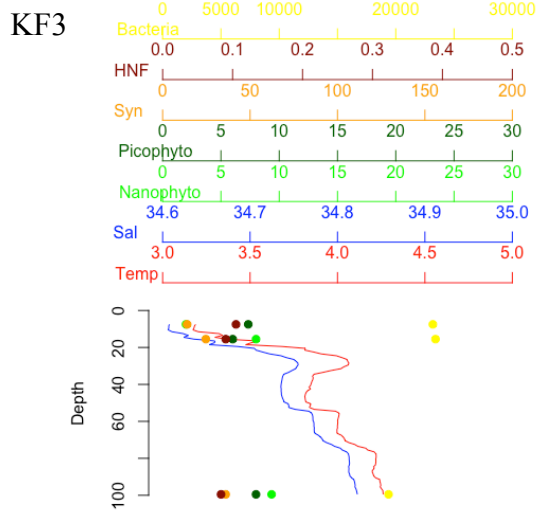
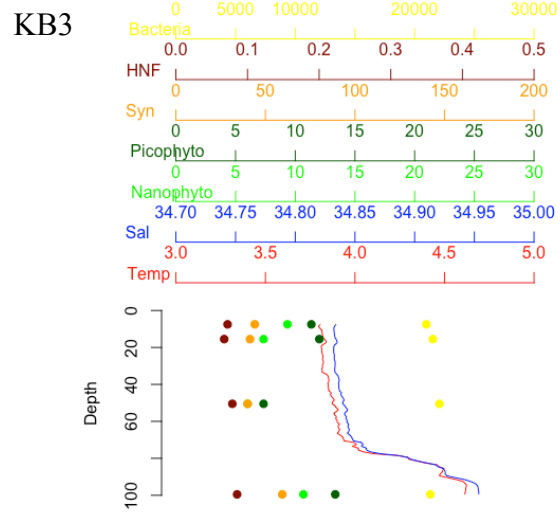
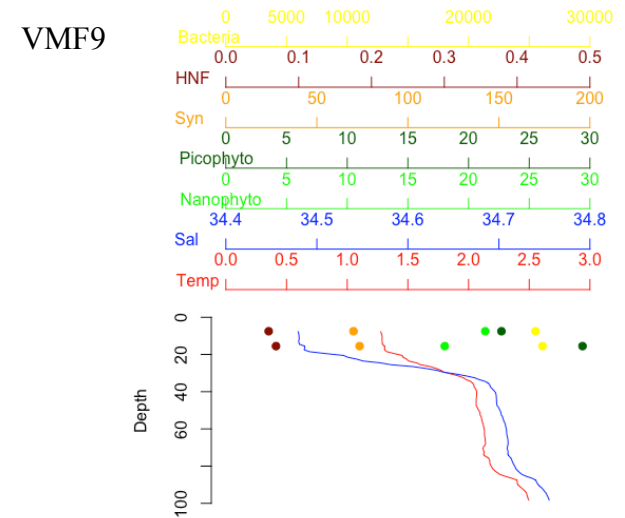
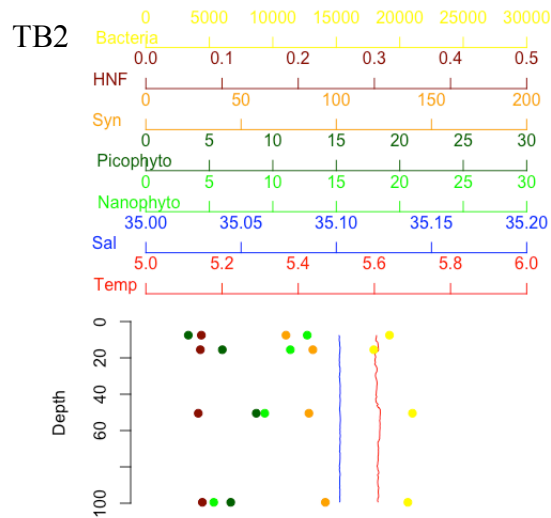
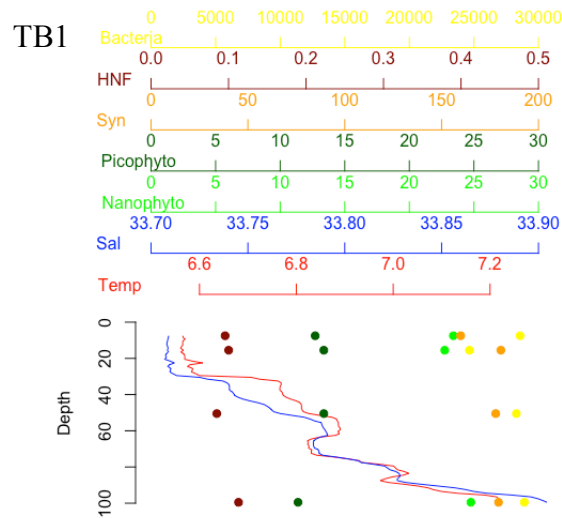
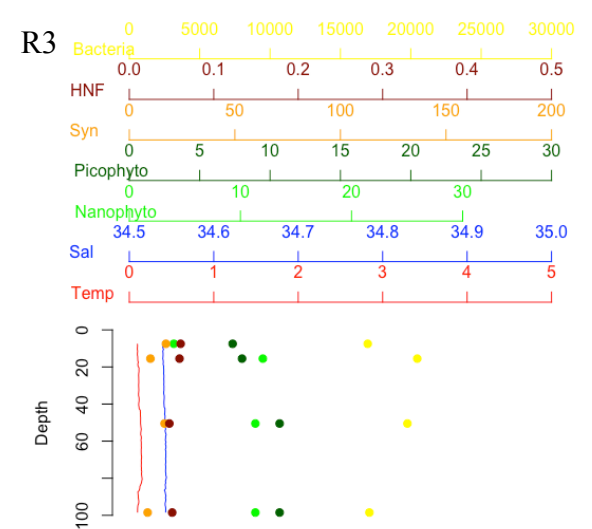
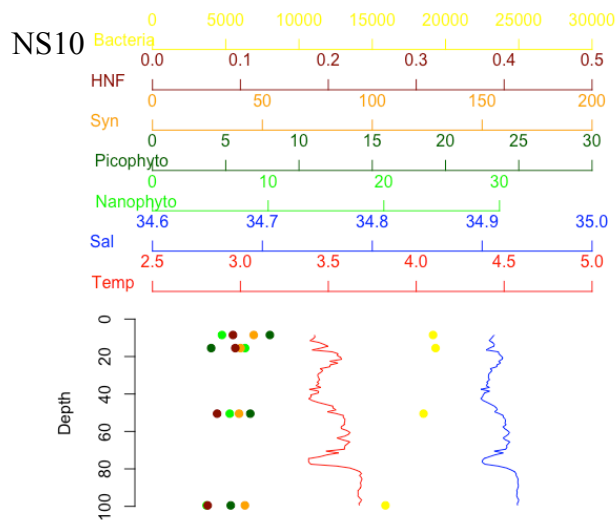
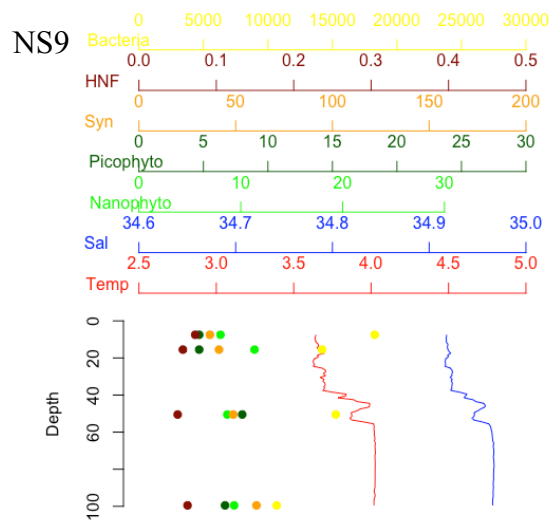
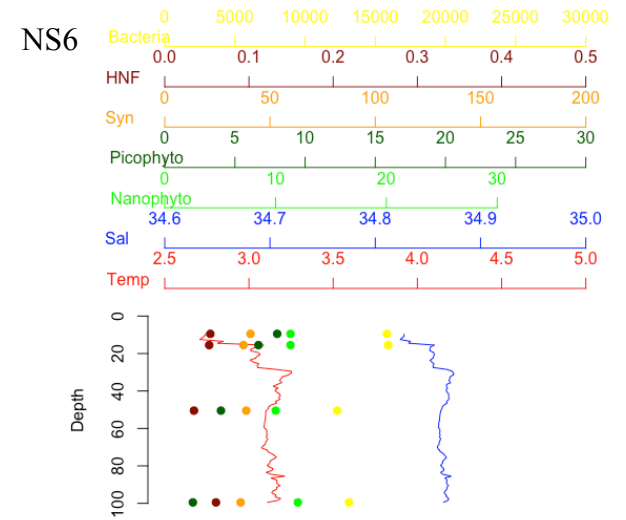
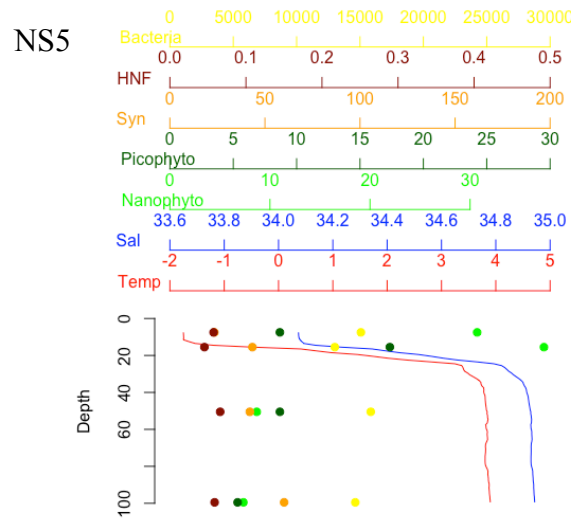
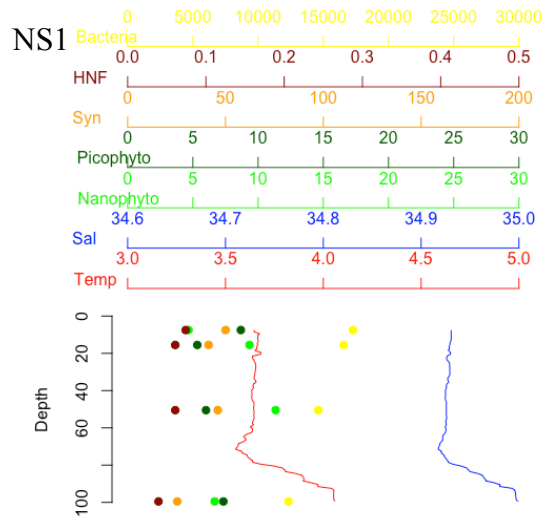
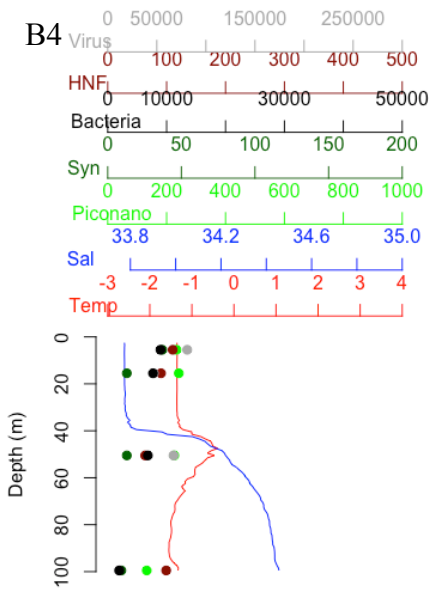
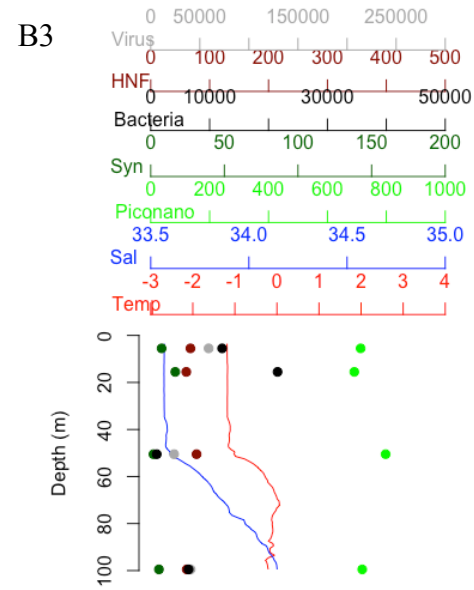
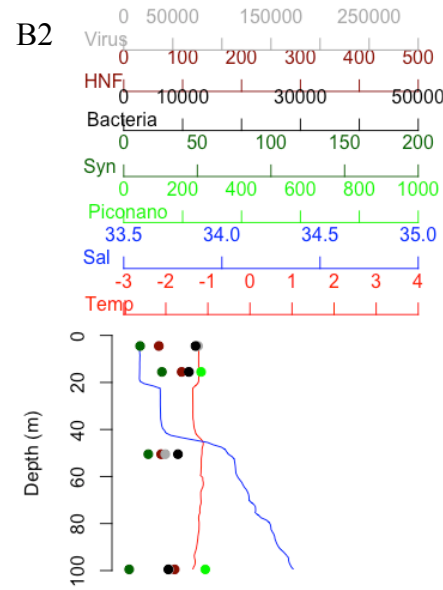
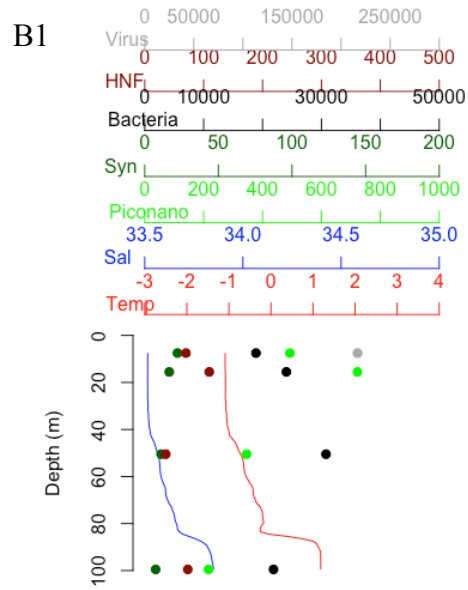
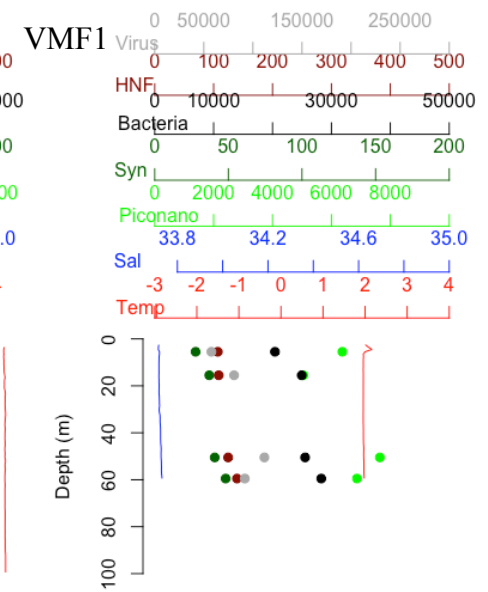
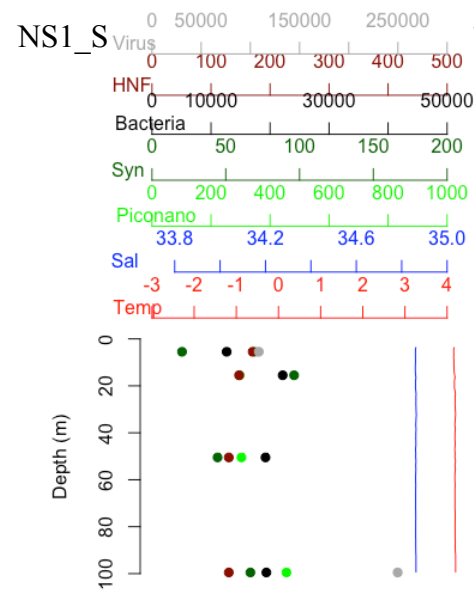
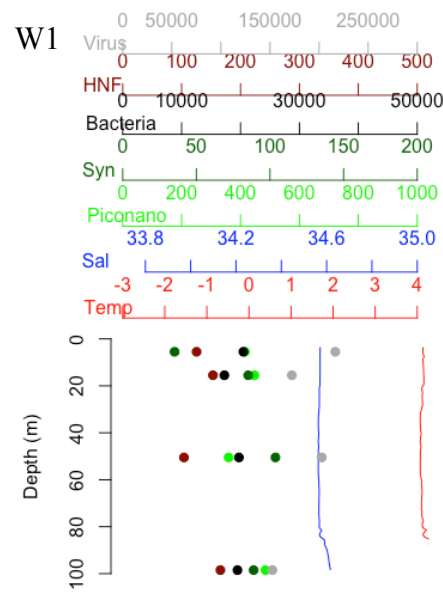
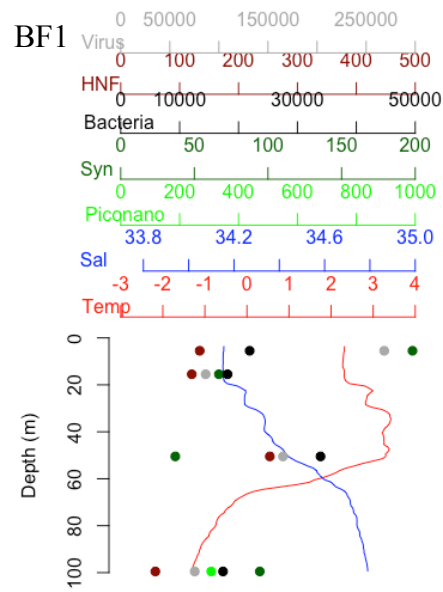


Figure 8 (continues over the next pages): vertical distribution of temperature, salinity and biological groups of interest throughout the first 100m of the water column in January and November. Each plot corresponds to a station sampled.





Multivariate analysis

Principal component analysis. A PCA was performed on the community abundances data. Applying the Kaiser criterion (retain the principal components with an eigenvalue greater than 1), two principal components PC1 and 2 were retained in January:

$$PC1 = 0.34 * Nanophyto + 0.29 * Picophyto + 0.46 * Syn + 0.39 * HNF + 0.47 * Bacteria + 0.46 * Viruses$$

$$PC2 = -0.55 * Nanophyto - 0.61 * Picophyto + 0.02 * Syn + 0.51 * HNF + 0.12 * Bacteria + 0.22 Viruses$$

These two components explained a very high fraction of the total variability of the data set (79.6%) with PC1 explaining 60.2% and PC 2 19.4%, respectively. The first component was positively associated with abundances of all groups, but with highest impact factors for heterotrophic bacteria (0.47) and cyanobacteria (Syn, 0.46). The second component was strongly positively correlated with HNF (0.51) and heterotrophic bacteria (0.12), and negatively linked to Pico- (-0.55) and Nanophytoplankton (-0.61); Cyanobacteria had little impact on PC2. The resulting PCA plots (Figure 9) for the individual water samples were analyzed both in the context of individual stations and based on previously defined hydrography criteria/water masses (see above). Based on water masses, samples from the NCC were clearly separated from the other stations by having higher abundances of most groups. The Atlantic Water stations had low PC1 values, indicating low overall organism abundance. However, the higher PC2 values indicate differentially higher abundances of HNF and bacteria making these stations more heterotrophically dominated. All Arctic Water samples were positioned equally along the PC1 axis, but exhibited a wider spread along PC2. The surface waters at NS5 (the only true Arctic Water station) were specifically characterized by higher abundances of autotrophic eukaryotic pico- and nanoplankton causing clear separation from deeper water samples from the same station along PC2. The “WSC” group showed no clear separation from the Arctic and Atlantic water communities. Looking at the grouping of the individual water samples (Figure 9), three subgroups can be distinguished: the two fjord stations KB3 and KF3 grouped closely with TB2, or the “Atlantic Water” group with medium (PC1) and high (PC2) values for the principle components. There was little to none overlap between this group and the stations along the NS transect north of Svalbard. The PCA also clearly demonstrated the unique community structure observed at TB1.

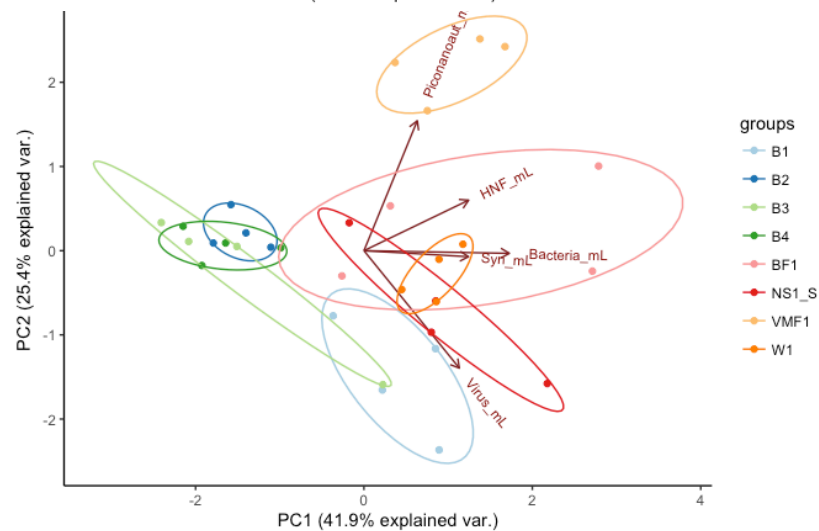
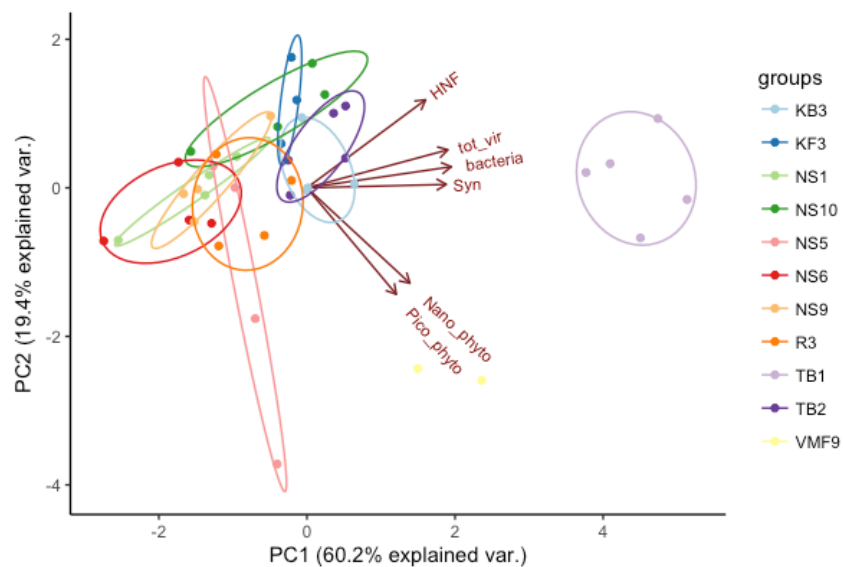
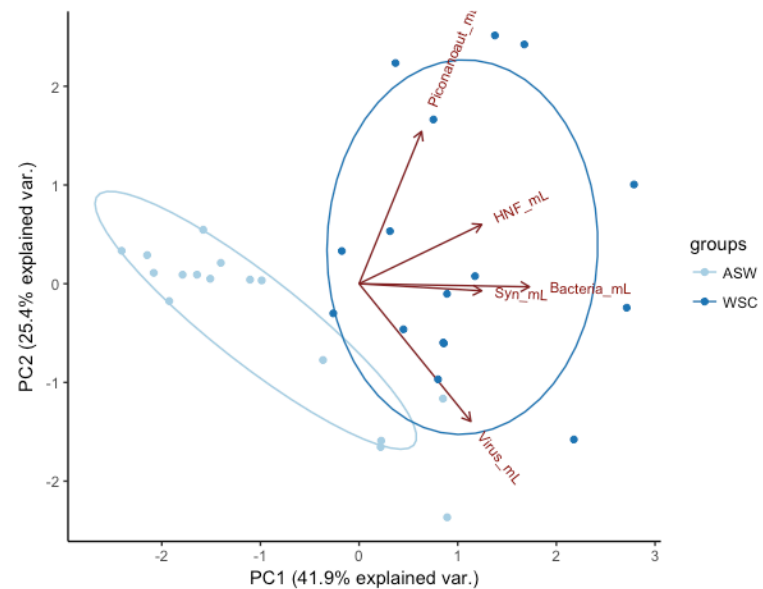
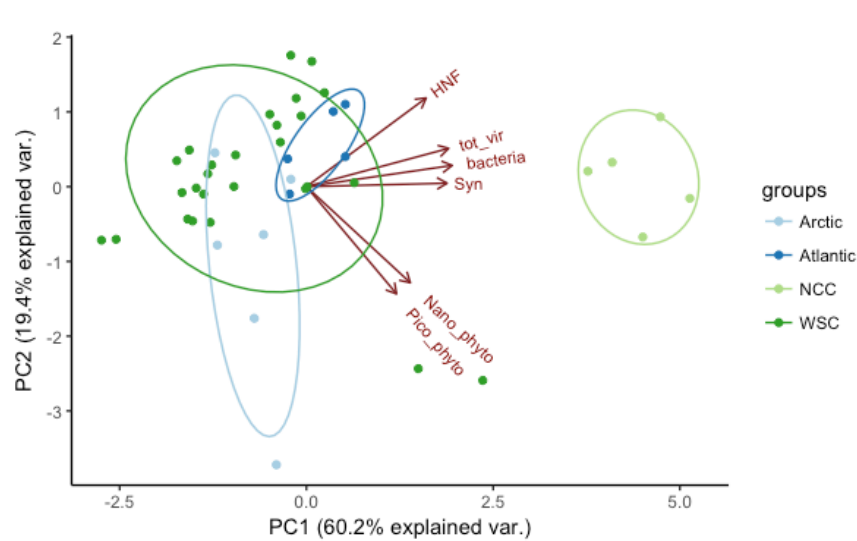


Figure 9: Principal Component Analysis performed on the abundance data in January (left) and November (right). Top: grouping according to water mass. Bottom: grouping by station.

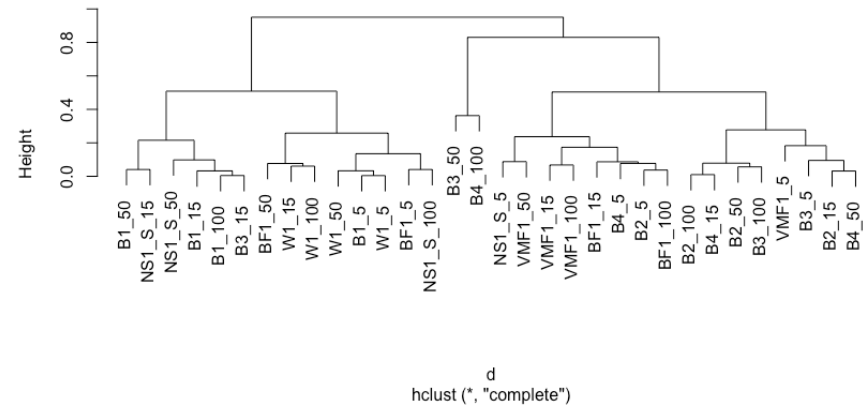
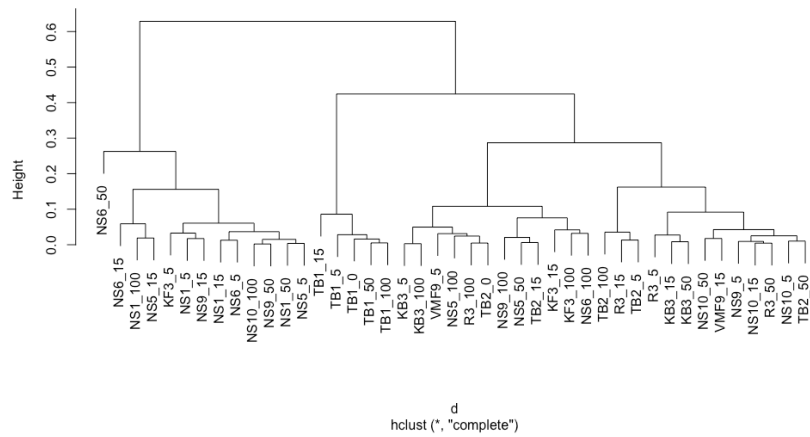
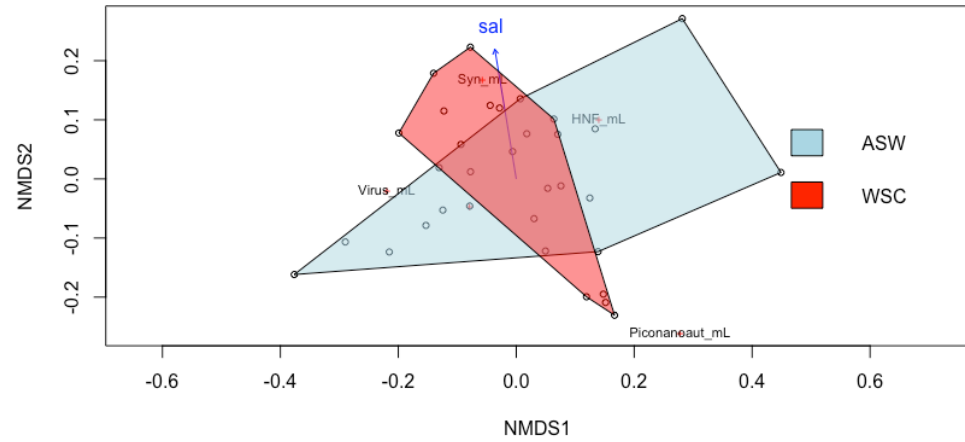
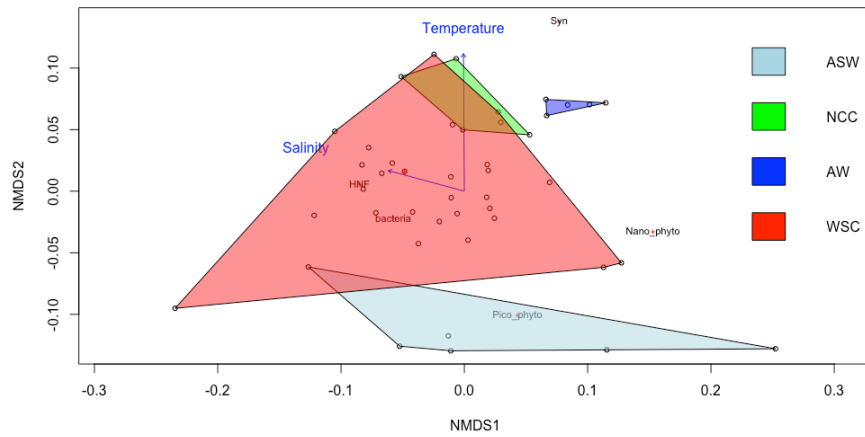


Figure 10: Top: Non-metric Multidimensional Scaling (NMDS) based on Bray-Curtis dissimilarity biplots for the January (left) and November (right) communities, with a stress of 0.12 and 0.13 respectively. Bottom: Cluster dendrograms based on Bray-Curtis dissimilarity (complete linkage method) for January and November.

The two retained principal components for the November data explained 41.9% and 25.4%, respectively of the total variance of the data set (67.3% cumulative variance explained).

$$PC1 = 0.23 * PicoNanophyto + 0.45 * Syn + 0.35 * HNF + 0.62 * Bacteria + 0.41 * Viruses$$

$$PC2 = 0.71 * PicoNanophyto - 0.03 * Syn + 0.28 * HNF - 0.014 * Bacteria - 0.64 * Viruses$$

Similar to the PCA from January, PC1 was positively related to the abundances of all groups, but strongest to heterotrophic bacteria (0.62), cyanobacteria (0.45), viruses (0.41) and HNF (0.35) (Figure 10). The second component PC2 was positively determined by the abundances of PNA (0.71) and negatively by viruses (-0.64). The resulting ordination in the PCA plot (Figure 10) showed a clear separation between water mass categories and between stations. Highest PC1 values indicating higher abundances of biota separated the Atlantic water samples from the more Arctic Barents Sea samples. Within the Barents Sea samples (B1 to B4), a separation can be seen of B1 with higher values of PC1 and lower PC2 values.

Non-metric Multidimensional scaling (NMDS). The results of the PCA for January are further supported in the NMDS ordination plot (Figure 10). The samples belonging to the Atlantic and NCC water masses are close to each other in this ordination (i.e. have a similar community structure in terms of abundances), and are distinguished from the rest by relatively higher abundances of *Synechococcus*. The inclusion of the variables temperature and salinity shows that these samples also align with higher temperatures along NMDS2 axis. Similarly, Arctic Water samples group on the opposite site along axis NMDS2. They are separated by colder temperatures and higher relative abundance of small-sized eukaryotic phytoplankton. Arctic Water samples are widespread along NMDS1 axis, showing that their community structure varied along with salinity differences. The “WSC” communities show a broad range of NMDS1 and 2 values and partially overlap with the NCC samples and one ASW sample. Overall the NMDS demonstrates that biological communities are grouped differently according to environmental conditions. The November NMDS show no clear separation according to environmental variables. Only salinity significantly influenced the ordination, likely through the more saline Atlantic Water mass with the corresponding higher abundance of *Synechococcus*.

Cluster dendrogram. The cluster analysis (Figure 10) for January supports the groupings observed in both the PCA and the NMDS biplots. Three clusters were distinguished. Cluster 1 contained all samples from Station TB1. The second cluster included most samples from the NS transect while the third cluster links most samples from the Barents Sea and Western fjords.

For November, no clear separation between samples based on hydrographical regime or location was observable, similar to the grouping results within the NMDS plot. This indicates a higher similarity between the communities throughout water masses.

Serial dilution experiments

There was no growth observed in any of the experiments by any of the studied groups (Figure 11). Apparent growth rates, which represent the balance of growth and mortality in terms of net change of population size, were overall very low and ranged between -0.025 and 0.025d^{-1} . In a serial dilution experiment, the intercept of the regression between said growth rates and the dilution factor is an estimate of the intrinsic growth of the cell population. In January, none of the intercepts was significantly different than 0 ($p > 0.05$). The same can be said for the November experiments, with the exception of Experiment 2, in which all groups displayed significantly negative growth rates, evidencing the decline of the populations ($p < 0.05$).

The slope of the regression lines (Figure 11) represents the grazing rate at which organisms are consumed (see “Materials and Methods”). None of the grazing rates estimated were significantly different from 0 ($p > 0.05$) in any experiment conducted during either January nor November. In summary nearly all serial dilution experiments demonstrated extremely low growth and/or grazing rates and no statistically significant results were obtained.

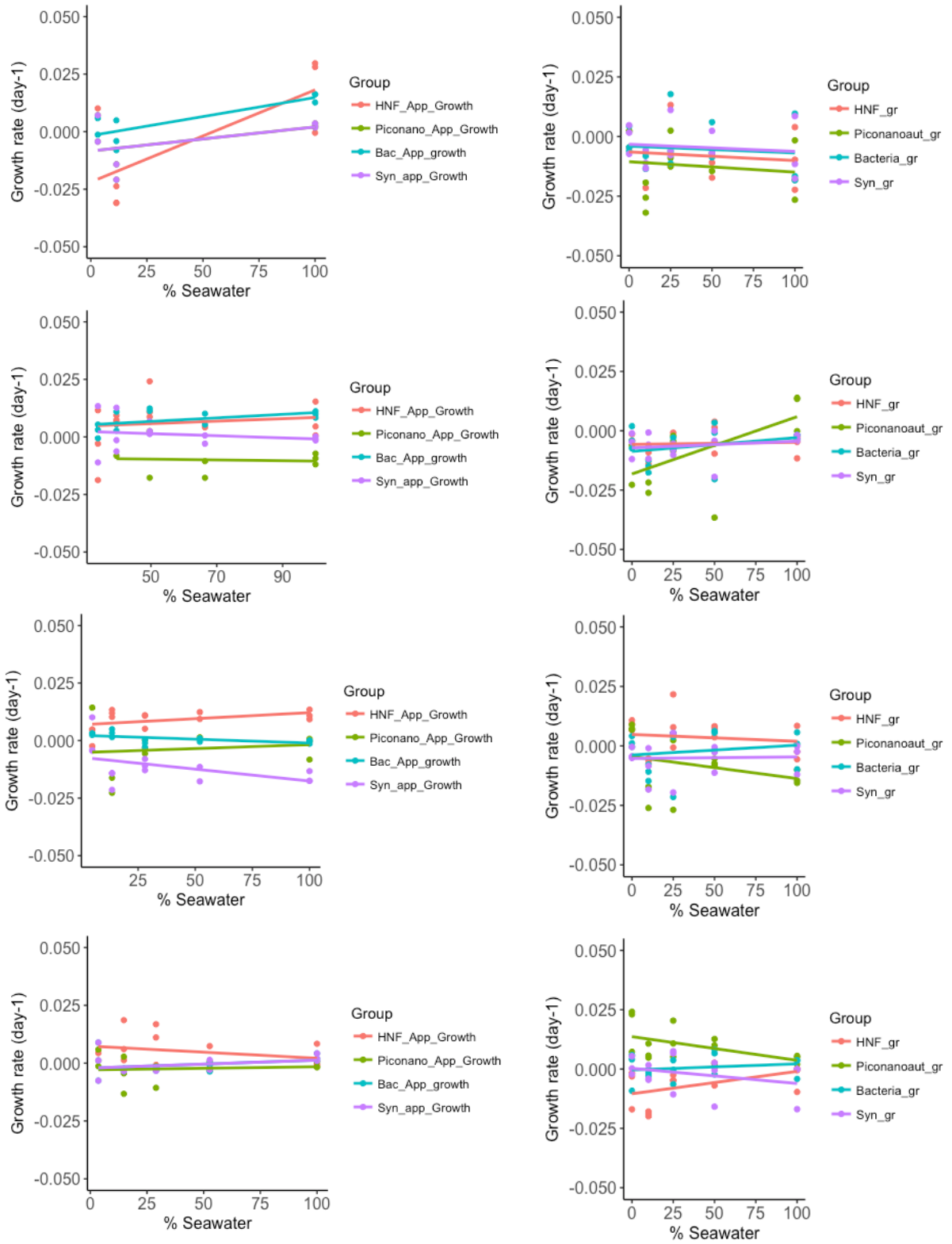


Figure 11: Apparent growth rates (d^{-1}) for the different groups in the serial dilution experiments. Left: January. Right: November.

Discussion

Physical oceanography

During the two expeditions the typical winter conditions for the main distinct water masses around Svalbard were encountered. The stations south of the archipelago were strongly influenced by the Atlantic Water transported northward in the North Atlantic Current and West Spitsbergen Current, which is characterized by relatively high temperatures and salinities (Cokelet et al., 2008). Atlantic Water was observed throughout the west and north coast of Spitsbergen, albeit in decreasing intensity along the West Spitsbergen Current. The fjords contained Atlantic Water that had been modified locally.

The southernmost station (TB1) was unique, as it had a clear influence by the Norwegian Coastal Current (NAC) causing a relatively lower salinity. This branch of the NAC does not differ in temperature from the northward flowing Atlantic Water, but has a reduced salinity most likely due to freshening by additions of river run-off along the coast of Norway (Skagseth et al., 2011).

The water masses encountered at the stations TB2 and W1 (in January and November, respectively) represented the core of Atlantic Water close to its gateway to the Arctic. Both stations were located offshore, so that local conditions (as in the fjords) did not alter temperature and salinity. However, each station is located towards the beginning and the end of the WSC, and this is reflected in the lower salinity of W1, as it carries the water added throughout Spitsbergen (Cokelet et al., 2008).

The fjords found along the western side of Svalbard are strongly influenced by the WSC. However, interannual variability (Nilsen et al. 2008) and regional scale geographic and climatic conditions cause differences between the fjords' hydrography compared to main body of AW and also for a high variability between them (Cottier et al. 2005). While the two more open or smaller fjords (stations KB3, KF3) were physically more similar to the AW, fjords with a sill or glacial inflow at its head diverged more. The regional modifications explain the differences between stations in van Mijenfjorden, with the innermost station VMF1 being much colder and fresher than VMF9. This difference is enhanced as VMF9 was located in the outer part of van Mijenfjorden west of Akseløya. This island emerges from a sill in the fjord and limits greatly the water exchange with its innermost parts, where VMF1 is located (Skardhamar & Svendsen

2010). Similarly, Billefjorden has a shallow sill and a relatively deep basin next to a glacier, which explain its overall colder waters compared to the core of the WSC. Moreover, the higher salinity and lower temperature in the deepest parts of BF1 can be explained by local cooling and sinking of cooled surface water and/or the additions of very cold and saline brine during periods of ice formation (e.g. Nilsen et al. 2008). The limited exchange between the WSC and a strong isolation of inner parts of the Billefjorden at BF1 is further supported by the low oxygen saturation values measured at depths below 40m (not reported here, in the cruise report for SIZE17).

North of Svalbard, the WSC has lost substantial heat, and it submerges due to its higher density underneath the fresher and colder Arctic Surface Water, that resides in the Central Arctic Ocean (Cokelet et al., 2008). Both measurements and model output high light the role of small scale eddies in this heat loss process in the WSC (Crews et al., 2017). The region of submergence of Atlantic Water north of Svalbard was closed studied during the NS1-10 transect, which crossed from the shelf to the shelf break and than back. Only on its northernmost station (NS5), we clearly observed submerged AW, separated by a pycnocline from surface ASW.

Contrastingly to the western side of Svalbard, Arctic Surface Water was sampled at all stations along the east coast. Most stations (except B1) demonstrated a stratification with ASW at the surface and warmer and more saline water below. This deeper water likely belongs to a branch of NAC that enters the Barents Sea and submerges below ASW at the Polar Front (Bluhm et al., 2015). The stations east of Svalbard were located north of the PF, and are thus dominated by ASW. The increasing temperature and salinity with depth can be attributed to the branch of the NAC. Specific conditions were observed at B1, where gradients were weakest. This indication of enhanced local mixing can be explained by the foramation of very strong gap flow winds generated in Hinlopen Strait (Barstad et al 2011).

Overall the hydrographic conditions at all stations were indicative of a seasonal cooling regime and strong mixing. Local exceptions at some stations could be explained by either the large scale regime (e.g. NS5) or the local hydrographic settings in fjords (e.g. BF1). Heat loss at the surface and wind generate turbulent mixing, which homogenizes the water column. This process allows the regeneration of nutrients and is key in the development of the phytoplankton bloom in spring (Sverdrup 1935).

The contrasting physical characteristics of these water masses, and the way they interact at a regional scale throughout the archipelago, were shown to be the drivers that shape the microbial communities in the area, as will be discussed in the following sections.

Photosynthetic pigments

Photosynthetic pigments, specifically Chlorophyll *a*, are widely used as indicators for the presence of primary producers in the marine environment. Seasonal changes in chlorophyll *a* have been used to describe the phenology of algal development in Arctic seas (Leu et al., 2015). Photosynthetic pigments were detectable in all stations, both in November and in January. These findings support the recent reports that indicate that the polar night is not devoid of autotrophic planktonic organisms (Rokkan Iversen & Seuthe, 2011; Hirche & Kosobokova, 2011; Vader & Marquardt, 2015).

Though detectable, Chlorophyll *a* concentrations were very low at all stations. Ranging between 0.01 and 0.05 µg/L, the values measured in this study are comparable to those reported throughout the Arctic during winter. Marquardt et al. (2016) found Chl*a* at a concentration of 0.04 µg/L in December and January at Isfjorden. Rokkan Iversen and Seuthe (2011) reported 0.01 µg/L in December in Kongsfjorden, and Hirche & Kosobokova (2011) measured 0.03 µg/L in Storfjord as late as March. These concentrations are orders of magnitude lower than those encountered during the spring bloom in the same areas: 8.1 µg/L (Marquardt et al 2016) or 9.9 µg/L (Rokkan Iversen & Seuthe 2011).

No significant difference was found between January and November in terms of Chl*a* concentration. However, both in November and in January, the pigment concentrations were higher in the Atlantic influenced stations. This suggests that advection of Chl*a* is an important term in the waters around Svalbard. Local photosynthetic production at this time of the year can be excluded due to the polar night regime. Integrated Chl*a* concentrations were not significantly different between or within months, and were comparable to the value of 5.3 mg/m² reported by Garneau et al (2008) in Franklin Bay (Canada) in winter.

Pheophytin is a breakdown product of Chl*a*, where the central Mg²⁺ ion is replaced by H⁺. It is mainly formed by biodegradation of Chl*a* during herbivory (e.g. Strom 1993). Pheophytin concentrations were significantly higher in November than in January, and again regionally higher in Atlantic Water samples. The regionally higher concentrations in the AW can again be explained by advective processes. As pheophytin is the degraded analog of Chl*a*, the higher

concentrations in November indicate remains of a late-autumn mortality of phytoplankton as well as herbivory and fecal pellet production by zooplankton that consume them (e.g. Strom 1993, Blachowiak-Samolyk et al. 2007).

The ratio of *Chla* to total pigments can be interpreted as a measure of the relative status of the phytoplankton communities. Actively growing communities e.g. during the Arctic spring bloom should have high ratios, while systems with low algal growth and dominance of herbivorous and senescence mortality should have low ratios. All ratios determined in this study did not exceed 0.5, clearly indicative of a winter situation with mostly degraded algal pigments. Interestingly we observed a significant higher ratio in November compared January. This indicates that the change from phototrophic to a heterotrophic dominated system still continued during the winter months, and that November and January conditions still differed from the standpoint of algal pigments although both systems were sampled during polar night conditions.

Abundances of pico- and nanoplankton

The distribution of microbial taxa showed clear regional patterns with big differences between different water masses and relations to local regimes, specifically in fjords and south of Hinlopen Strait. Contrastingly, little evidence for vertical distribution patterns were observed as indicative a very active mixing regime in the study area in November and January. I will thus focus in the following discussion on the regional patterns for all microbial taxa studied.

Eukaryotic Pico-Nanoautotrophs. November pico-nanophytoplankton abundances were similar between stations except for the very high values at VMF1. Similar to shifts in the pigment concentrations (being more heterotrophic), January abundances were 2 orders of magnitude lower than in those in November indicating a substantial reduction in the abundance of the pico- and nanoautotrophic cells. Similar to November, the van Mijenfjord station VMF9 had highest values in January. This indicates that local regimes can have a high influence on the abundance of pico- and nanophytoplankton. This is further supported by the very high variability of reported cell abundances from various parts of the Arctic. Literature values for winter were highly variable: 230 ± 230 cells/mL in the central Arctic Ocean (Sherr & Sherr, 2003), and 56 – 153 cells/mL in December, Franklin Bay (Vaqué et al., 2008), and an integrated value of $2 \cdot 10^{12}$ cells/m² (Rokkan Iversen & Seuthe, 2011) in December, Kongsfjorden. This study suggests that regional differences within the Arctic make it important to study on a

regional scale, and that significant changes occur during the polar winter period between the months of November and January.

Cyanobacteria. Picoplankton sized cyanobacteria of the genus *Synechococcus* are important primary producers in many parts of the world's oceans but have been reported only in low abundances from Arctic seas (e.g. Gradinger and Lenz 2005). Both in January and in November, *Synechococcus* abundances were greater in the Atlantic influenced waters. This supports the concept that *Synechococcus* is mainly advected to the Arctic, including Svalbard with the northwards moving Atlantic Water and in the WSC (Gradinger and Lenz 2005, Lund Paulsen et al., 2017). In contrast to many temperate oceans, *Synechococcus* is not the dominating picoautotroph in the Arctic Ocean, where the niche is occupied by *Micromonas* (Not et al., 2005) potentially due to unique adaptations of *Micromonas* to the Arctic living conditions, specifically in winter (McKie-Krisberg and Sanders 2014).

The observed seasonal difference in abundance of cyanobacteria were also found by Lund Paulsen et al. (2017) with 51 cells/mL in January and 600 ± 250 cells/mL in November. Their slightly higher November abundances can be explained by the combination of the advective nature of the cyanobacterial populations and the interannual variability in the influx of AW through the NAC (Cokelet, 2008).

Heterotrophic Nanoflagellates. Heterotrophic nanoflagellates have been highlighted as key contributors to the microbial food webs due their role as major consumers of pelagic bacteria (e.g. Rokkan Iversen & Seuthe, 2011). Still, surprisingly few studies have focused on their abundances in Arctic waters, and specifically in the winter season. The regionally higher abundances in Atlantic water can be attributed to water mass advection. The observed January abundances in this study were much lower than those reported from other parts of the Arctic or Kongsfjorden with values of 260 ± 80 cells/mL for the central Arctic (Sherr & Sherr 2003), 21-72 cells/mL for Franklin Bay (Vaqué et al., 2005), and an integrated value of $2 \cdot 10^9$ cells/m² for Kongsfjorden (Rokkan Iversen & Seuthe, 2011), while the November data overlapped with the previously mentioned abundance values from other studies. Again, substantial abundance decreases were found comparing November and January data and regionally higher abundances in Atlantic Water samples compared to Arctic waters. The strong seasonal reduction of HNF during the study season can not be directly explained by the loss of light, as they rely mainly on bacterial food. However bacterial production is often closely tied to algal primary production, which again would explain the reduced abundances of HNF in November and the further decrease towards January.

Heterotrophic bacteria. Bacteria play a key role in the recycling of dissolved organic matter in the pelagic realms of the Arctic as part of the microbial loop (e.g. Saint-Beat et al. 2018). Their sensitivity study on an Arctic ecosystem model actually indicated that Arctic food webs might be most sensitive on the level of bacterial production. Consequently, studies of bacterial activity and abundance are relevant not only in warm parts of the oceans as earlier suggested but also in Arctic seas. During our two expeditions, bacterial abundances remained rather constant throughout the dark season, and were consistently one order of magnitude below data from other Arctic studies for the same season with values of $2.4 \pm 1 \cdot 10^5$ cells/mL (Vaqué et al., 2008), $1.8 \pm 0.3 \cdot 10^5$ cells/mL (Sherr & Sherr, 2003), and an integrated value of $14 \cdot 10^{12}$ cells/m² (Rokkan Iversen & Seuthe 2011). Potential reasons for the low abundances could be in low substrate availability for growth and loss due to grazing or viral lysis (Vaqué et al. 2008). On a regional scale, bacterial abundances were consistently highest in Atlantic Water, suggestion a similar role of advection as seen for other microbial functional groups. The notable exception was station B1 in the Barents Sea, which substantially higher abundances than the more southerly stations B2-4. As discussed above, B1 was located south of Hinlopen Strait, where strong winds develop and could cause vertical mixing and the potential of resuspension of sedimented organisms. This could either lead to enhanced substrate availability for pelagic bacteria, or increase of bacterial abundances by additions of benthic forms.

Viruses play a very important part in microbial food webs as major cause of bacterial lysis. They can be the primary cause of bacterial mortality exceeding grazing losses due to heterotrophic flagellates (Wells and Demming 2006). Despite their apparent importance, their presence and activity in polar seas is very poorly studied, specifically in the polar night. Overall, viral abundances followed a nearly identical regional distribution pattern with their bacteria, exceeding bacterial values by a factor of roughly 10. This values agrees with early reported VBR (Virus to Bacteria Ratio) for the surface waters in the Arctic of approximately 10 (Suttle, 2007). Modeling studies by Winter et al. (2012) suggest a close relation between bacterial and viral abundances with decreasing values related to decreasing day length and decreasing temperatures. This agrees with our observations.

Multivariate community analysis

The various multivariate analysis techniques applied in this study confirmed the strong linkages between abundances of the microbial food web components and the physical characteristics of the water mass. The patterns that emerged in the Principal Component Analysis were consistent throughout both months: PC1 (which represented the highest degree of variability in the entire

data set) was strongly influenced by the abundances of most groups, while PC2 could be interpreted as a “autotrophic versus heterotrophic” axis (PNA vs. HNF in January and PNA vs. viruses in November). In this common ordination space, abundances of most taxa were highest in Atlantic Water influenced samples in line with the strong advective signal discussed already above. The relevance of water masses as important factors was also supported in the resulting biplots and through the cluster analysis. When comparing November and January biplots, the better separation in November and the larger overlap in the January biplot are likely due to the lack of sufficient Arctic Surface Water sampling in the January cruise.

The NMDS plots support this hypothesis. In both months, NMDS shows that *Synechococcus* was highly associated with warmer and/or more saline waters likely due to advection in Atlantic Water (Gradinger and Lenz 2005, Lund Paulsen et al. 2017). While advection certainly applies to other taxa as well, relatively higher abundances of pico- and nanoautotrophs occurred in the ASW samples which had typically been colder and fresher.

Some distinct differences between the November and January abundance data were found. In terms of abundances, PNA and HNF abundances in November were orders of magnitude higher than in January. While their abundances seemed to decrease during the polar night, abundances for heterotrophic bacteria and viruses remained constant and *Synechococcus* increased in Atlantic Water. The combination of these observations suggests this novel hypothesis of a succession within the microbial food web during the polar night:

Advection of Atlantic Water seeds the waters around Svalbard in relatively uniform and high abundances of microbial taxa. As winter progresses, the strong physical and substrate limitations act as bottleneck and advected taxa that are not adapted to the local Arctic winter conditions decrease in abundance. The seasonal decrease in pico-nanophytoplankton and reduced bacterial production due to substrate limitation lead to reduced abundances of heterotrophic flagellates. Heterotrophic bacteria may die or survive in an inactive stage for months (e.g. Manini and Danovaro, 2006), whereas a switch to mixotrophy can support *Synechococcus* and the eukaryotic pico-nanoautotrophs through the dark season (see next section). This can lead to a reset of the entire systems to a new start for the “spring-bloom” succession when sufficient light returns to the system.

This hypothesis can be explored in future studies. One possible approach would be the application of metagenomics to detect shifts in taxonomic composition throughout the season as already successfully applied by Wilson et al. (2017). Moreover, metatranscriptomics and/or

metaproteomics could be employed to search for the seasonally shifting expression of genes responsible for e.g. spore formation, nitrogen fixation and/or mixotrophic enzymes.

Serial dilution experiments

Several serial dilution experiments were conducted with the aim to get detailed insights into the dynamics of the microbial food web. As was mentioned in the “Results” section, the dilution experiments did not show the expected results. Typically, higher dilutions should have decreased the encounter rate between predator and prey and increase the growth rates of e.g. bacteria (Landry & Hassett 1981). Under such conditions, the intercept of the fitted line with the y-axis would provide the specific growth rate, and the slope of the regression line the grazing rate. However, in almost all of the experiments conducted in this project these lines were practically flat (a slope of 0) and crossed the y-axis at near-0 or even negative values. It is obvious from these results that some of the basic assumptions of the serial dilution experiments were not met, or that this methodology was not sensitive enough to determine the desired rate due to very long generation times. One possible explanation would be inactivity or very low activity rates of most members of the microbial community in the polar night. This assumption has support from some field studies that observed very slow growth rates of bacteria during the polar night, with reported bacterial growth rates of $<0.1 \text{ d}^{-1}$ (Rokkan Iversen & Seuthe, 2011) and 0.03 d^{-1} (Sherr & Sherr 2003). Vaqué et al. (2008) could determine carbon based growth rate for bacteria ($0.19 \pm 0.38 \mu\text{g CL}^{-1} \text{ d}^{-1}$), which were compensated by very similar grazing rates ($0.16 \pm 0.7 \mu\text{g CL}^{-1} \text{ d}^{-1}$). Moreover, only a very small fraction (1-2%) of a winter bacterial community in Franklin Bay was active based on staining with CTC (5-Cyano-2,3-ditolyl tetrazolium chloride, a stain for determine active versus inactive bacteria) going down to 0.1% during mixing events (Lovejoy et al. 1996). These observations provide strong evidence that low activity might have caused the outcome of the experiments.

However, mixotrophy could further complicate the applied scenario by adding trophic pathways to the the “classical” trophic relationships in the planktonic food web. Indeed, ingestion experiments demonstrated that mixotrophic pico- and nanoplankton can play a significant role in bacterivory in early autumn (Sanders & Gast 2018). This pathway seems even more relevant to Svalbard waters as both *Micromonas* (by phagotrophy) and *Synechococcus* (by osmotrophy) can shift to mixotrophy (McKie-Krisberg & Sanders 2014, Yelton et al. 2016). This strategy for the dark season was also proposed as a survival mechanism for small phytoflagellates by Zhang et al. (1998).

The combination of low activity rates and shifting trophic relationships are likely causes to explain the difficulty in applying the serial dilution approach to the polar night conditions.

Methodological considerations

Sampling during the polar night regime provides unique challenges with working under often harsh environmental conditions specifically freezing temperatures and no light. Sampling efforts can easily be biased by inadequate sample handling like exposure to light, which has the potential to alter biological activity even at low light levels as demonstrated recently for zooplankton (e.g. Ludvigsen et al. 2017). Greatest care was taken to minimize such light exposure. Sampling occurred basically on a dark ship with all investigators wearing red headlamps. During filling of bottles, all tubings and samples were secured against light by dark tape. The further processing of samples and setting up of the experiments occurred in a dark lab with limit light coming from a red headlamp. While small light contamination might have occurred over periods of few seconds during the entire handling processes, complete darkness had been secured for the major part of the sample treatment and experimental duration.

Sampling times. Sampling was not possible within the same winter period. Therefore, the two sampling events were separated by ca 10 months in 2017. While interannual variability in physical variables can contribute to year to year variation within the same months, , we argue that from a biological point of view, the strong environmental factor light, governing the major phenology of biological processes in the Arctic Ocean (e.g. Leu et al. 2015) allows for a direct comparison of November and January data as representatives for these months, neglecting interannual differences. This study suggest that the duration of the dark and substrate limited season is the major cause for the observed differences.

Flow cytometry. Only a limited set of approaches can be used to determine the abundances of all major contributors of the microbial network in the same samples. In addition to flow cytometry, quantification of cell abundances could have been done by light microscopy employing settling chambers or epifluorescence microscopy. Both of these techniques are widespread in literature and often used in combination (e.g. Paulsen et al., 2017, Felip et al., 2007) but come with their specific limitations. Light microscopy was not suitable for the goals of this study because the groups of interest are too small for its resolution power. Flow cytometry was chosen over epifluorescence microscopy because of its recorded consistent abundance estimates of all members of the microbial community.

Different flow cytometers were employed to analyze the samples from November and January, which could entail a systematic bias in the measurements. To minimize this, the sampling and laboratory procedures were reproduced with exhaustive attention and all measurements were supervised and/or conducted by the same operator (me).

Serial dilution experiments. Because low growth rates were expected, the experimental incubations were handled with the utmost care to make sure that the organisms were not exposed to light they are sensitive to, which would elicit a confounding response. All steps of the experimental setup and sampling took place in the dark, with the use of only red headlamps, and temperature was recorded during incubation. Excessive stirring of the water was also avoided when transferring volumes between containers to prevent cell disturbance. Furthermore, greatest care was taken to minimize differences in the dilution of replicates.

As stated in the “Methods section”, the experiments conducted in January were not sampled for time-0 blank controls, which decidedly poses an issue when estimating rates. However, the estimates used for these concentrations were observed to not be very sensitive to small variations in the generation time of the organisms, and they were later corroborated by similar results in the following set of experiments. Given the expected low generation times, experiments were run for several days, while higher growth and grazing rates allow in most more temperature or Arctic summer studies to obtain significant results within 24 hour incubations (e.g. Serena Fonda & Alfred 2003). In the outlook section I suggest several alternative approaches that could be applied during the polar night season to gather specific insights into the seasonality of microbial communities during the polar night.

Conclusions and outlook

All major functional groups of the microbial network exist in the waters around Svalbard during the dark season in November and in January as suggested by earlier Arctic studies. All major groups (viruses, heterotrophic bacteria, cyanobacteria, heterotrophic nanoflagellates and autotrophic pico- and nanoflagellates) were present in all samples in abundances comparable to other studies. Clear regional distribution patterns were detected mostly related to water mass structure. Advection by the incoming Atlantic water appears to be an important process.

I propose that a succession in the microbial food web is taking place throughout the polar night period, fueled by the advection of organisms and shaped by the bottleneck imposed by the severe Arctic conditions. As winter progresses, overall abundances of nano-sized organisms decrease, but a tight community of winter-adapted pico-sized biota remains. A useful toolset to characterize these communities and prove or reject this hypothesis would be metaomics, as has already been performed in the area.

No evidence of active growth or predation was found in the studied communities. It remains to be cleared whether this is due to a suboptimal experimental approach or if it actually reflects the picture of a persistent but dormant community. A simple methodological addition would be to quantify the fraction of active bacterial and eukaryotic cells by diagnostic staining and microscopy counts. Applying this technique to feeding experiments would also allow to observe if nanoflagellates exert any preferences in their diet over dead or live prey. Furthermore, attempting to assess the possible mixotrophic activity of cyanobacteria or eukaryotic phytoplankton would help understand their survival throughout the dark months.

Overall, these findings open a pathway for additional studies during the polar night with potential impacts on the planktonic dynamics of the rest of the year and its resilience towards future natural or anthropogenic disturbances.

References

- Alonso-Sáez, L., Sánchez, O., Gasol, J. M., Balagué, V., & Pedrós-Alio, C. (2008). Winter-to-summer changes in the composition and single-cell activity of near-surface Arctic prokaryotes. *Environmental Microbiology*, *10*(9), 2444–2454. <https://doi.org/10.1111/j.1462-2920.2008.01674.x>
- Alonso-Saez, L., Waller, A. S., Mende, D. R., Bakker, K., Farnelid, H., Yager, P. L., ... Bertilsson, S. (2012). Role for urea in nitrification by polar marine Archaea. *Proceedings of the National Academy of Sciences*, *109*(44), 17989–17994. <https://doi.org/10.1073/pnas.1201914109>
- Angly, F. E., Felts, B., Breitbart, M., Salamon, P., Edwards, R. A., Carlson, C., ... Rohwer, F. (2006). The marine viromes of four oceanic regions. *PLoS Biology*, *4*(11), 2121–2131. <https://doi.org/10.1371/journal.pbio.0040368>
- Azam, F., & Graf, J. S. (1983). The Ecological Role of Water-Column Microbes in the Sea. *Marine Ecology Progress Series*, *10*, 257–263.
- Berge, J., Cottier, F., Last, K. S., Varpe, Ø., Leu, E., Søreide, J., ... Brierley, A. S. (2009). Diel vertical migration of Arctic zooplankton during the polar night. *Biol. Lett*, *5*, 69–72. <https://doi.org/10.1098/rsbl.2008.0484>
- Berge, J., Renaud, P. E., Darnis, G., Cottier, F., Last, K., Gabrielsen, T. M., ... Falk-Petersen, S. (2015). In the dark: A review of ecosystem processes during the Arctic polar night. *Progress in Oceanography*, *139*, 258–271. <https://doi.org/10.1016/j.pocean.2015.08.005>
- Blachowiak-Samolyk, K., Kwasniewski, S., Dmoch, K., Hop, H., & Falk-Petersen, S. (2007). Trophic structure of zooplankton in the Fram Strait in spring and autumn 2003. *Deep-Sea Research Part II: Topical Studies in Oceanography*, *54*(23–26), 2716–2728. <https://doi.org/10.1016/j.dsr2.2007.08.004>
- Bluhm, B. A., Kosobokova, K. N., & Carmack, E. C. (2015). A tale of two basins: An integrated physical and biological perspective of the deep Arctic Ocean. *Progress in Oceanography*, *139*(August), 89–121. <https://doi.org/10.1016/j.pocean.2015.07.011>
- Burn, Chris. *The Polar Night* (1996). The Aurora Research Institute. Retrieved April 2018
- Børsheim, K. Y. (2017). Bacterial and primary production in the Greenland Sea. *Journal of Marine Systems*, *176*(August), 54–63. <https://doi.org/10.1016/j.jmarsys.2017.08.003>

- Calbet, A., Calbet, A., & Saiz, E. (2015). The Ciliate-Copepod Link in Marine Ecosystems The ciliate-copepod link in marine ecosystems, *38*(FEBRUARY 2005), 157–167. <https://doi.org/10.3354/ame038157>
- Christaki, U. (2001). Nanoflagellate predation on auto- and heterotrophic picoplankton in the oligotrophic Mediterranean Sea. *Journal of Plankton Research*, *23*(11), 1297–1310. <https://doi.org/10.1093/plankt/23.11.1297>
- Coachman, A. L. K., & Barnes, C. A. (2018). Surface Water in the Eurasian Basin of the Arctic Ocean Published by: Arctic Institute of North America Stable URL : <http://www.jstor.org/stable/40507022> Linked references are available on JSTOR for this article : SURFACE WATER IN THE EURASIAN BASIN, *15*(4), 251–278.
- Cokelet, E. D., Tervalon, N., & Bellingham, J. G. (2008). Hydrography of the West Spitsbergen Current, Svalbard Branch: Autumn 2001. *Journal of Geophysical Research: Oceans*, *113*(1), 1–16. <https://doi.org/10.1029/2007JC004150>
- Cottier, F., Tverberg, V., Inall, M., Svendsen, H., Nilsen, F., & Griffiths, C. (2005). Water mass modification in an Arctic fjord through cross-shelf exchange: The seasonal hydrography of Kongsfjorden, Svalbard. *Journal of Geophysical Research: Oceans*, *110*(12), 1–18. <https://doi.org/10.1029/2004JC002757>
- Crews, L., Sundfjord, A., Albrechtsen, J., & Hattermann, T. (2018). Mesoscale Eddy Activity and Transport in the Atlantic Water Inflow Region North of Svalbard. *Journal of Geophysical Research: Oceans*, *123*(1), 201–215. <https://doi.org/10.1002/2017JC013198>
- Cronin, H. A., Cohen, J. H., Berge, J., Johnsen, G., & Moline, M. A. (2016). Bioluminescence as an ecological factor during high Arctic polar night. *Scientific Reports*, *6*(April), 1–9. <https://doi.org/10.1038/srep36374>
- Eckerstorfer, M., & Christiansen, H. H. (2017). The “ High Arctic Maritime Snow Climate ” in Central Svalbard Author (s): Markus Eckerstorfer and Hanne H . Christiansen Source : Arctic , Antarctic , and Alpine Research , Vol . 43 , No . 1 (February 2011), pp . 11-21 Published by : INSTAAR , Univers, *43*(1), 11–21. <https://doi.org/10.1657/1938-4246-43.1.11>
- Felip, M., Andreatta, S., Sommaruga, R., Straskrábová, V., & Catalan, J. (2007). Suitability of flow cytometry for estimating bacterial biovolume in natural plankton samples: Comparison with microscopy data. *Applied and Environmental Microbiology*, *73*(14), 4508–4514. <https://doi.org/10.1128/AEM.00733-07>

- Frainer, A., Primicerio, R., Kortsch, S., Aune, M., Dolgov, A. V., Fossheim, M., & Aschan, M. M. (2017). Climate-driven changes in functional biogeography of Arctic marine fish communities. *Proceedings of the National Academy of Sciences*, *114*(46), 201706080. <https://doi.org/10.1073/pnas.1706080114>
- Garneau, M.-È., Roy, S., Lovejoy, C., Gratton, Y., & Vincent, W. F. (2008). Seasonal dynamics of bacterial biomass and production in a coastal arctic ecosystem: Franklin Bay, western Canadian Arctic. *Journal of Geophysical Research*, *113*(C7), C07S91. <https://doi.org/10.1029/2007JC004281>
- Gradinger, R., & Lenz, J. (1995). Seasonal occurrence of picocyanobacteria in the Greenland Sea and central Arctic Ocean. *Polar Biology*, *15*(6), 447–452. <https://doi.org/10.1007/BF00239722>
- Grenvald, J. C., Callesen, T. A., Daase, M., Renaud, P. E., Cottier, F., & Grenvald, J. C. (2016). Plankton community composition and vertical migration during polar night in Kongsfjorden, 1879–1895. <https://doi.org/10.1007/s00300-016-2015-x>
- Greenacre, M., & Primicerio, R. (2013). *Multivariate Analysis of Ecological Data: Chapter 13*. Fundación BBVA, Barcelona
- Grotefendt, K., Logemann, K., Quadfasel, D., & Ronski, S. (1998). Is the Arctic Ocean warming? *Journal of Geophysical Research*, *103*(C12), 27679. <https://doi.org/10.1029/98JC02097>
- Hirche, H. J. (1997). Life cycle of the copepod *Calanus hyperboreus* in the Greenland Sea. *Marine Biology*, *128*(4), 607–618. <https://doi.org/10.1007/s002270050127>
- Hirche, H. J., & Kosobokova, K. N. (2011). Winter studies on zooplankton in Arctic seas: The Storffjord (Svalbard) and adjacent ice-covered Barents Sea. *Marine Biology*, *158*(10), 2359–2376. <https://doi.org/10.1007/s00227-011-1740-5>
- Holm-Hansen, O., & Riemann, B. (1978). *Nordic Society Oikos Chlorophyll a Determination : Improvements in Methodology* Author (s): Osmund Holm-Hansen and Bo Riemann Published by: Wiley on behalf of Nordic Society Oikos Stable URL : <http://www.jstor.org/stable/3543338> REFERENCES Linked refere, *30*(3), 438–447. Retrieved from doi:10.2307/3543338
- Iversen, K. R., & Seuthe, L. (2011). Seasonal microbial processes in a high-latitude fjord (Kongsfjorden, Svalbard): I. Heterotrophic bacteria, picoplankton and nanoflagellates.

- Polar Biology*, 34(5), 731–749. <https://doi.org/10.1007/s00300-010-0929-2>
- Kosobokova, K. N. (1999). The reproductive cycle and life history of the Arctic copepod *Calanus glacialis* in the White Sea, 254–263.
- Landry, M. R., & Calbet, A. (2018). Microzooplankton production in the oceans, 507(March). <https://doi.org/10.1016/j.icesjms.2004.03.011>
- Landry, M. R., & Hassett, R. P. (1982). Estimating the grazing impact of marine microzooplankton. *Marine Biology*, 67(3), 283–288. <https://doi.org/10.1007/BF00397668>
- Last, K. S., Hobbs, L., Berge, J., Brierley, A. S., & Cottier, F. (2016). Moonlight Drives Ocean-Scale Mass Vertical Migration of Zooplankton during the Arctic Winter. *Current Biology*, 26(2), 244–251. <https://doi.org/10.1016/j.cub.2015.11.038>
- Leu, E., Mundy, C. J., Assmy, P., Campbell, K., Gabrielsen, T. M., Gosselin, M., ... Gradinger, R. (2015). Arctic spring awakening - Steering principles behind the phenology of vernal ice algal blooms. *Progress in Oceanography*. <https://doi.org/10.1016/j.pocean.2015.07.012>
- Ludvigsen M, Berge J, Geoffroy M, Cohen JH, De La Torre PR, Nornes SM, Singh H, Sørensen AJ, Daase M, Johnsen G (2017) Use of an Autonomous Surface Vehicle reveal new zooplankton behavioral patterns and susceptibility to light pollution during the polar night. *Science Advances* 4, eaap9887. DOI: 10.1126/sciadv.aap9887.
- Manini, E., & Danovaro, R. (2006). Synoptic determination of living/dead and active/dormant bacterial fractions in marine sediments. *FEMS Microbiology Ecology*, 55(3), 416–423. <https://doi.org/10.1111/j.1574-6941.2005.00042.x>
- Marquardt, M. (2016). Marine microbial eukaryotes in Svalbard waters: Seasonality, community composition and diversity. Retrieved from Munin in April 2018.
- McKie-Krisberg, Z. M., & Sanders, R. W. (2014). Phagotrophy by the picoeukaryotic green alga *Micromonas*: Implications for Arctic Oceans. *ISME Journal*, 8(10), 1953–1961. <https://doi.org/10.1038/ismej.2014.16>
- Nilsen, F., Cottier, F., Skogseth, R., & Mattsson, S. (2008). Fjord-shelf exchanges controlled by ice and brine production: The interannual variation of Atlantic Water in Isfjorden, Svalbard. *Continental Shelf Research*, 28(14), 1838–1853. <https://doi.org/10.1016/j.csr.2008.04.015>

- Paulsen, M. L., Doré, H., Garczarek, L., Seuthe, L., Müller, O., Sandaa, R.-A., ... Larsen, A. (2016). Synechococcus in the Atlantic Gateway to the Arctic Ocean. *Frontiers in Marine Science*, 3(October), 191. <https://doi.org/10.3389/fmars.2016.00191>
- Pree, B., Kuhlisch, C., Pohnert, G., Sazhin, A. F., Jakobsen, H. H., Lund Paulsen, M., ... Larsen, A. (2016). A simple adjustment to test reliability of bacterivory rates derived from the dilution method. *Limnology and Oceanography: Methods*, 14(2), 114–123. <https://doi.org/10.1002/lom3.10076>
- Ryther, J. H. (1969). Photosynthesis and fish production in the sea. *Science*, 166(3901), 72-76.
- Saint-Béat, B., Maps, F., & Babin, M. (2018). Unraveling the intricate dynamics of planktonic Arctic marine food webs. A sensitivity analysis of a well-documented food web model. *Progress in Oceanography*, 160(January), 167–185. <https://doi.org/10.1016/j.pocean.2018.01.003>
- Sanders, R. W., & Gast, R. J. (2018). Bacterivory by phototrophic picoplankton and nanoplankton in Arctic waters, 82(March), 242–253. <https://doi.org/10.1111/j.1574-6941.2011.01253.x>
- Sarmiento, H., Montoya, J. M., Vázquez-Domínguez, E., Vaqué, D., & Gasol, J. M. (2010). Warming effects on marine microbial food web processes: how far can we go when it comes to predictions? *Philosophical Transactions of the Royal Society of London. Series B, Biological Sciences*, 365, 2137–2149. <https://doi.org/10.1098/rstb.2010.0045>
- Serena Fonda, U., Alfred, B. 2003. Seasonal variations in the dynamics of microbial plankton communities: first estimates from experiments in the Gulf of Trieste, Northern Adriatic Sea. *Marine Ecology Progress Series*, 247: 1-16.
- Sherr, E. B., Sherr, B. F., Wheeler, P. A., & Thompson, K. (2003). Temporal and spatial variation in stocks of autotrophic and heterotrophic microbes in the upper water column of the central Arctic Ocean. *Deep-Sea Research Part I: Oceanographic Research Papers*, 50(5), 557–571. [https://doi.org/10.1016/S0967-0637\(03\)00031-1](https://doi.org/10.1016/S0967-0637(03)00031-1)
- Skagseth, O., Drinkwater, K. F., & Terrile, E. (2011). Wind-and buoyancy-induced transport of the Norwegian Coastal Current in the Barents Sea. *Journal of Geophysical Research: Oceans*, 116(8). <https://doi.org/10.1029/2011JC006996>
- Skarðhamar, J., & Svendsen, H. (2010). Short-term hydrographic variability in a stratified Arctic fjord. *Geological Society, London, Special Publications*, 344(1), 51–60.

<https://doi.org/10.1144/SP344.5>

- Strom, S. L. (1993). Production of pheopigments by marine protozoa: results of laboratory experiments analysed by HPLC. *Deep-Sea Research Part I*, 40(1), 57–80. [https://doi.org/10.1016/0967-0637\(93\)90053-6](https://doi.org/10.1016/0967-0637(93)90053-6)
- Suttle, C. A. (2007). V lo Marine viruses — major players in the global ecosystem, 5. <https://doi.org/10.1038/nrmicro1750>
- Terrado, R., Lovejoy, C., Massana, R., & Vincent, W. F. (2008). Microbial food web responses to light and nutrients beneath the coastal Arctic Ocean sea ice during the winter – spring transition. *Journal of Marine Systems*, 74(3–4), 964–977. <https://doi.org/10.1016/j.jmarsys.2007.11.001>
- R Core Team (2013). R: A language and environment for statistical computing. R Foundation for Statistical Computing, Vienna, Austria. URL <http://www.R-project.org/>.
- Thingstad, T. F., Bellerby, R. G. J., Bratbak, G., Børsheim, K. Y., Egge, J. K., Heldal, M., ... Neill, C. (2008). Counterintuitive carbon-to-nutrient coupling in an Arctic pelagic ecosystem, 455(September). <https://doi.org/10.1038/nature07235>
- Vader, A., & Marquardt, M. (2015). Key Arctic phototrophs are widespread in the polar night, 13–21. <https://doi.org/10.1007/s00300-014-1570-2>
- Vaqué, D., Guadayol, Ò., Peters, F., Felipe, J., Angel-Ripoll, L., Terrado, R., Lovejoy, C., et al. 2008. Seasonal changes in planktonic bacterivory rates under the ice-covered coastal Arctic Ocean. *Limnology and Oceanography*, 53: 2427–2438.
- Vihtakari, M., Welcker, J., Moe, B., Chastel, O., Tartu, S., Hop, H., ... Gabrielsen, G. W. (2018). Black-legged kittiwakes as messengers of Atlantification in the Arctic. *Scientific Reports*, 8(1), 1–11. <https://doi.org/10.1038/s41598-017-19118-8>
- Wasmund, N., Topp, I., & Schories, D. (2006). Optimising the storage and extraction of chlorophyll samples. *Oceanologia*, 48(1), 125–144.
- Wells, L. E., & Deming, J. W. (2006). Modelled and measured dynamics of viruses in Arctic winter sea-ice brines. *Environmental Microbiology*, 8(6), 1115–1121. <https://doi.org/10.1111/j.1462-2920.2006.00984.x>
- Wilson, B., Müller, O., Nordmann, E., Seuthe, L., & Bratbak, G. (2017). Changes in Marine Prokaryote Composition with Season and Depth Over an Arctic Polar Year, 4(April), 1–

17. <https://doi.org/10.3389/fmars.2017.00095>

Winter, C., Payet, J. P., & Suttle, C. A. (2012). Modeling the Winter-to-Summer Transition of Prokaryotic and Viral Abundance in the Arctic Ocean. *PLoS ONE*, 7(12). <https://doi.org/10.1371/journal.pone.0052794>

Yelton, A. P., Acinas, S. G., Sunagawa, S., Bork, P., Pedrós-alió, C., & Chisholm, S. W. (2016). Global genetic capacity for mixotrophy in marine picocyanobacteria, 2946–2957. <https://doi.org/10.1038/ismej.2016.64>

Zhang, Q., Gradinger, R., & Spindler, M. (1998). Dark Survival of Marine Microalgae in the High Arctic (Greenland Sea). *Polarforschung*, 65(3), 111–116. <https://doi.org/10.2312/polarforschung.65.3.111>